

Optimization of the Small Scale Expression of the Mutant Hen Egg White Lysozyme,  
H15S

by

Charles Duah Amoyaw

Submitted in Partial Fulfillment of the Requirements  
for the Degree of Master of Science  
in the Chemistry Program

Youngstown State University

May 2020

I hereby release this thesis to the public. I understand this thesis will be made available from the OhioLINK ETD Center and the Maag Library Circulation Desk for public access. I also authorize the University or other individuals to make copies of this thesis as required for scholarly research.

Signature:

---

*Charles Duah Amoyaw*, Student

Date

Approvals:

---

*Michael Serra, Ph.D.*, Thesis Advisor

Date

---

*Nina Stourman, Ph.D.*, Committee Member

Date

---

*John Jackson, Ph.D.*, Committee Member

Date

---

*Dr. Sal Sanders, Ph.D.*, Dean of Graduate Studies

Date

## ABSTRACT

Reactive oxygen species (ROS) are chemically reactive oxygen containing molecules and radicals mainly produced from the partial reduction of molecular oxygen. ROS have been associated with aging and several diseases such as atherosclerosis and cancer. Metal-catalyzed oxidation (MCO) systems are systems that produce free radicals using transition metal ions such as copper or iron and hydrogen peroxide. As such, MCO may cause oxidation of proteins. To study the correlation between protein structure and oxidative damage of proteins by MCOs, different mutants of hen egg white lysozyme (HEWL) have been developed. This research focuses on the optimization of the expression of the mutant HEWL H15S. The *Pichia pastoris* expression system was adapted for the expression of HEWL H15S. The *P. pastoris* X-33-pPICZ $\alpha$ A-*hewl*H15S strain was subjected to different growth conditions in a glycerol and methanol buffered media under conditions for small scale expression. Both intracellular and extracellular protein expression were analyzed for enzyme activity. Increasing glycerol concentration from 0.5% to 1% did not show significant increase in yeast growth resulting in low protein concentration and enzyme activity at 28 °C. Also, protein expression at three different methanol concentrations at 28 °C: 0.5% (v/v), 1% (v/v), and 2% (v/v) showed an increase in enzyme activity but only small changes in total protein concentration. The addition of calcium chloride showed a significant effect on the expression of H15S to about 1mg/mL compared to the other conditions without CaCl<sub>2</sub>. Lysing of the cells grown at 28 °C for intracellular analysis by the Bradford assay showed a significant band of protein corresponding to the size of the H15S mutant. A lower temperature of 22 °C at different growth and expression conditions measured high protein concentration and an increase in

enzyme activity for extracellular expression. Intracellular analysis on protein expression at 22 °C measured no lysozyme activity.

## **ACKNOWLEDGEMENTS**

First of all, I would like to acknowledge with gratitude the support, dedication and guidance of my advisor, Dr. Michael Serra throughout my entire years at YSU. He was always attentive to details and kept me on my toes to get the work done. I like to thank my committee members, Dr. Nina Stourman and Dr. John Jackson for their time and been patience with the revisions of my thesis. In addition, I would like to thank Dr. Doug Genna for being very inspirational and encouraging through my one year of knowing him.

Secondly, I would especially like to thank my lovely wife, Angela Kwarkoh and my son NanaYaw Duah Amoyaw, for being supportive and putting up with me for being away from them through my years of studies. I thank my mom and my sisters who kept calling from Ghana with their words of encouragement.

Finally, I would like to thank the YSU College of Graduate Studies and the YSU Chemistry Department for making this a possibility with their financial support and curriculum.

## Table of Contents

SECTION	PAGE #
Title Page	i
Signature Page	ii
Abstract	iii
Acknowledgements	v
Table of Contents	vi
Table of Figures	ix
Table of Equations	xii
Table of Tables	xiii
List of Abbreviation	xiv
Introduction	1
Free Radicals	1
Reactive Oxygen	1
Anti-Oxidants	3
Oxidative Damage	6
Reactive Oxygen Mediated Modification of Proteins	7
Reactive Oxygen Species Signal Transduction	11
Metal Catalyzed Oxidation (MCO) Systems	14
Site specific oxidation and Protein Oxidation	16
Lysozyme	17
<i>Pichia pastoris</i> and pPICZαA <sup>®</sup>	18

Research Statement	20
Materials and Methods	21
Materials	21
Instrumentation	21
Preparation of YPD Plates	22
Buffered Glycerol-Complex Medium (BMGY) + caa + EDTA	22
Buffered Methanol-Complex Medium (BMMY)	22
Growth of Yeast Strains	23
Small Scale Expression of a Hen Egg White Lysozyme Mutant (HEWL H15S)	23
Ammonium Sulfate Fractionation	24
Bradford Assay	24
SDS-PAGE	25
Enzyme Assay	26
Intracellular Analysis of Cell Pellets by SDS-PAGE	27
Optimization of <i>Pichia pastoris</i> Protein Expression	28
Results	30
The Effect of pH on the Growth of <i>P. pastoris</i> X-33-pPICZ $\alpha$ A- <i>hewl</i> H15S	30
The Effect of Methanol Concentration on the Extracellular Expression of HEWL H15S	30
Bradford Assay	33
SDS-PAGE	35
Enzyme Assay	35
Growth at 28 °C and Precipitation at Different Ammonium Sulfate Concentrations	36

Bradford Assay	38
SDS-PAGE	39
Enzyme Assay	41
The Effect of Glycerol Concentration on the Growth of <i>P. pastoris</i> X-33-pPICZαA-hewlH15S	40
Protein Expression and Concentration	43
Bradford Assay	44
<i>SDS-PAGE</i>	45
Enzyme Assay	50
Intracellular Expression	49
SDS-PAGE	49
Extracellular Expression vs. Intracellular Expression at 22 °C	50
Extracellular Expression of Pelleted Cells.	50
Enzyme Assay of Intracellular vs. Extracellular Expression	58
Discussion	59
Conclusion	65
References	66



## Table of Figures

FIGURE TITLE	PAGE #
1.1. The general scheme of the reduction of O <sub>2</sub> to produce water with the reactive oxygen species intermediates the superoxide anion, hydrogen peroxide, and the hydroxyl radical.	1
1.2. The Lewis structures of oxygen, the hydroxyl ion, and some common reactive oxygen species.	2
1.3. The Fenton Reaction	3
1.4. The Haber-Weiss Reaction	3
1.5. The neutralization of ROS by antioxidants	5
1.6. A free radical scavenging mechanism by the NADPH-glutathione Reductase (GR) system	5
1.7. Presumable scheme of ischemia-induced free radical generation and tissue damage	7
1.8. Possible scheme for the oxidation of the peptide chain	8
1.9. Possible schemes leading to peptide bond cleavage by the $\alpha$ -amidation and diamide pathway.	9
1.10. An OH <sup>•</sup> attack on the side chains of glutamyl residues results in peptide bond cleavage	10
1.11. An OH <sup>•</sup> attack on the side chains of prolyl residues results in peptide bond cleavage	10
1.12. Possible schemes for H <sub>2</sub> O <sub>2</sub> -dependent signal transduction	13
1.13. A possible mechanism for the site-specific metal ion-catalyzed oxidation of proteins by a “caged type” reaction	15
1.14. A site specific oxidation by a copper MCO system on amyloid- $\beta$ peptide (A $\beta$ ) in the presence of ascorbate (Asc)	16
1.15. A picture of HEWL’s tertiary structure	18
1.16. A picture of the pPICZ $\alpha$ plasmid	19

3.1.	A plot of absorbance at 595 nm vs $\mu\text{g}$ [BSA]	31
3.2A.	SDS-PAGE for 0.5% MeOH concentration condition of the fractions collected in 24 h time intervals to 96 h	34
3.2B.	SDS-PAGE for 1% MeOH concentration condition of the fractions fractions collected in 24 h time interval to 96 h	35
3.3.	SDS-PAGE of the 96 h supernatant fractions expressed in either 0.5% (v/v) or 1% (v/v) MeOH and precipitated at either 65% or 65-85% $(\text{NH}_4)_2\text{SO}_4$	38
3.4.	SDS-PAGE of the supernatant fraction precipitated at 85% - 100% ammonium sulfate	39
3.5.A.	Growth curve of <i>P. pastoris</i> X33-pPICZ $\alpha$ A- <i>hewlH15S</i> grown in 0.5% (v/v) GY monitored as OD <sub>600</sub> with time. Midpoint growth time was 13 h	41
3.5.B.	Growth curve of <i>P. pastoris</i> X33-pPICZ $\alpha$ A- <i>hewlH15S</i> grown in 1% (v/v) GY monitored as OD <sub>600</sub> with time. Midpoint growth time was 17 h	42
3.6A.	SDS-PAGE analysis of aliquots collected from 24 to 96 h of <i>P. pastoris</i> X33-pPICZ $\alpha$ A- <i>hewlH15S</i> strain initially expressed in BMGY media at 0.5% (v/v) GY with protein expression in BMMY at 1% (v/v) MeOH	44
3.6B.	SDS-PAGE analysis of aliquots collected from 24 to 96 h of <i>P. pastoris</i> X33-pPICZ $\alpha$ A- <i>hewlH15S</i> strain initially expressed in BMGY media at 0.5% (v/v) GY with protein expression in BMMY at 2% (v/v) MeOH	45
3.6C.	SDS-PAGE analysis of aliquots collected from 24 to 96 h of <i>P. pastoris</i> X33-pPICZ $\alpha$ A- <i>hewlH15S</i> strain initially expressed in BMGY media at 1% (v/v) GY with protein expression in BMMY at 1% (v/v) MeOH	46
3.6D.	SDS-PAGE analysis of aliquots collected from 24 – 96 h of <i>P. pastoris</i> X33-pPICZ $\alpha$ A- <i>hewlH15S</i> strain initially expressed in BMGY media at 1% (v/v) GY with protein expression in BMMY at 2% (v/v) MeOH	47
3.7.	A histogram of presentation of [Protein] $\times 10^3$ (mg/mL) and enzyme activity (Units/mg).	48
3.8.	SDS-PAGE of supernatant samples obtained from lysing cells grown at 0.5% (v/v) GY from 24 to 96 hours were analyzed using a	49

Mini-PROTEAN<sup>®</sup> TGX<sup>™</sup> 8-16% ready-made gel from Bio-Rad.

3.9A.	SDS-PAGE of supernatant of lysed cells at 24 h time intervals from 24 to 96 h and initially grown at either 0.5% (v/v) or 1% (v/v) MeOH + CaCl <sub>2</sub> - EDTA	50
3.9B.	SDS-PAGE of supernatant of lysed cells at 24 h time intervals from 24 to 96 h and initially grown at 0.5% (v/v) MeOH + CaCl <sub>2</sub> + EDTA	51
3.10A.	SDS-PAGE of extracellular fractions at 24 h time intervals from 24 to 96 h with protein expression in either 0.5% (v/v) or 1% (v/v) MeOH + CaCl <sub>2</sub> - EDTA	53
3.10B.	SDS-PAGE of extracellular fractions at 24 h time intervals from 24 to 96 h with protein expression at 0.5% (v/v) MeOH + CaCl <sub>2</sub> + EDTA	54
3.10C.	SDS-PAGE of extracellular fractions at 24 h time intervals from 24 to 96 h with protein expression at 0.5% (v/v) MeOH - CaCl <sub>2</sub> + EDTA	55
3.11.	SDS-PAGE aliquots from <i>P. pichia</i> plus pPICZ $\alpha$ A Control	58

## Table of Equations

<b>TITLE</b>	<b>PAGE #</b>
2.I. Equation to determine the percent protein concentration of lysozyme	27
2.II. Equation to determine units/mg of enzyme in reaction mixture	28
2.III. Equation to determine mg enzyme in reaction mixture	28

## Table of Tables

TITLE	PAGE #
1.1. Oxidation products of amino acids	11
1.2. Types of MCO Systems	14
3.1. Optical Density at 600nm of yeast culture grown in BMGY, pH 5	30
3.2. Bradford Assay of supernatant fractions grown in either 0.5% (v/v) or 1% (v/v) MeOH collected at 24 h intervals from 24 to 96 hours	32
3.3. Determination of enzyme activity of samples grown either 0.5% (v/v) or 1% (v/v) MeOH and at 28 °C	36
3.4. Bradford Assay on 96 h growth fractions initially grown in either 0.5% (v/v) or 1% (v/v) MeOH. The protein was precipitated at 65% or 65-85% ammonium sulfate concentration	37
3.5. Determination of enzyme activity of 96 h fractions grown at either 0.5% (v/v) or 1% (v/v) MeOH precipitated at different ammonium sulfate concentrations	40
3.6. The growth of <i>P. pastoris</i> X33-pPICZ $\alpha$ A- <i>hew</i> /H15S in either 0.5% (v/v) or 1% (v/v) glycerol was monitored as OD <sub>600</sub> with time	41
3.7. Bradford assay results for protein expressed with either 0.5% (v/v) or 1% (v/v) GY concentration and different concentration of MeOH- either 1% (v/v) or 2% (v/v)	43
3.8. Turbidimetric enzyme assay of 96 h fractions for samples grown at different GY% and MeOH concentrations	48
3.9. Turbidimetric enzyme assays of intracellular fractions at 24 h intervals from 24 to 96 h from yeast grown at 0.5% (v/v) GY and different EDTA, CaCl <sub>2</sub> and MeOH concentrations.	52
3.10. Determination of extracellular protein concentration expressed from yeast cells grown at 22 °C with varying growth conditions of EDTA, CaCl <sub>2</sub> and MeOH concentration	56
3.11. Turbidimetric enzyme assays of extracellular fractions at 24 h intervals from 24 to 96 h grown at 0.5% (v/v) GY and different EDTA, CaCl <sub>2</sub> and MeOH concentrations.	57

## List of Abbreviations and Molecules

Abs, A	Absorbance
ATP	Adenosine triphosphate
A $\beta$	amyloid- $\beta$ peptide
Å	Angstrom
Asc	Ascorbate
B	Biotin
BSA	Bovine Serum Albumin
BMGY	Buffered Glycerol-complex Medium
BMMY	Buffered Methanol-complex Medium
caa	Casamino Acid
DI	deionized
DNA	Deoxyribonucleic Acid
DHA	Dehydroascorbate
D	Dextrose
EDTA, E	ethylenediaminetetraacetic Acid
GPX	Glutathione Peroxidase
GR	Glutathione Reductase
GY	Glycerol
Hs, h, hs	Hour(s)
ROOH	Hydroperoxide
HEWL	Hen Egg White Lysozyme
kD	kiloDalton

MCO	Metal-Catalyzed Oxidation
MeOH	Methanol
μg	Microgram
μL	Microliter
mL	Milliliter
mg	Milligram
mM	Millimolar
MES	2-(N-Morpholino)ethanesulfonic Acid
nm	Nanometer
NADPH	Nicotinamide adenine dinucleotide phosphate
OD	Optical Density
PRX	Peroxiredoxin
pH	Potential Hydrogen
KPi	Potassium Phosphate Buffer
ROS	Reactive Oxygen Species
GSH	Reduced Glutathione
rpm	Revolution per minute
s	Seconds
SDS	Sodium Dodecyl Sulfate
SDS-PAGE	Sodium Dodecyl Sulfate-Polyacrylamide Gel Electrophoresis
O <sub>2</sub> <sup>•-</sup>	Superoxide
SOD	Superoxide Dismutase
UV-Vis	Ultraviolet -Visible

V	Volts
× g	relative centrifugal force
YPD	Yeast Extract Peptone Dextrose Medium
YNB	Yeast Nitrogen Base



## CHAPTER 1: INTRODUCTION

### Free Radicals

A radical (usually known as a free radical) is defined as an atom or set of atoms with single or multiple unpaired electrons. Free radicals can be negatively or positively charged or uncharged. Radicals are mainly produced as intermediates in different biological and chemical processes and are highly reactive due to their unpaired electrons. This property describes their biological activities and ability to cause damage to macromolecules and cells when they are manufactured excessively or inefficiently managed.<sup>1</sup>

### Reactive Oxygen Species

Reactive oxygen species (ROS) are chemically reactive oxygen containing molecules, ions, and radicals. Oxygen contains two unpaired electrons in separate orbitals in its outermost shell. In view of this electronic configuration, oxygen is more susceptible to form radicals. ROS are formed by the reduction of oxygen and they include the superoxide anion, hydrogen peroxide and the hydroxyl radical. **Figures 1.1** and **1.2** represent the reduction of oxygen to produce the most common reactive oxygen species as intermediates and their Lewis structures respectively.<sup>2</sup>

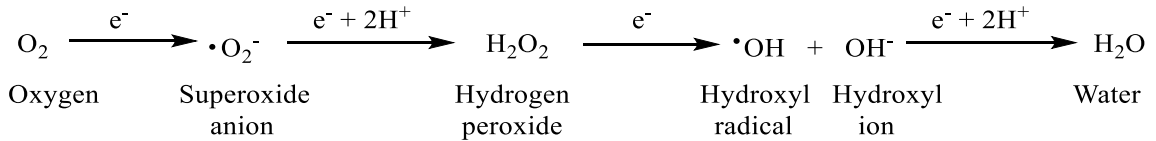


**Figure 1.1:** The general scheme of the reduction of O<sub>2</sub> to produce water with the reactive oxygen species intermediates the superoxide anion, hydrogen peroxide, and the hydroxyl radical.

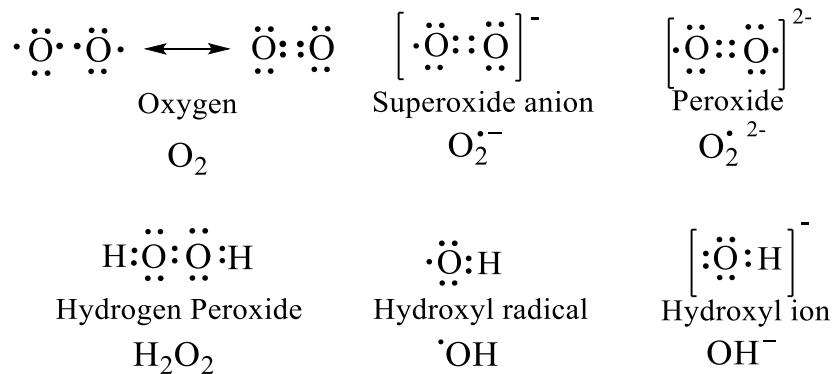


**Figure 1.2:** The Lewis structures of oxygen, the hydroxyl ion and some common reactive oxygen species. Each structure is labeled with its name and chemical formula. The • represents an electron.

ROS can be generated in a variety of ways in biological systems. They can be formed both endogenously and exogenously. They are produced endogenously during electron transport in the mitochondria from the partial reduction of  $\text{O}_2$  through electron leakage, during the respiratory burst, and during inflammation. ROS can be formed from exogenous mechanisms which include ionizing radiation, smoking, and xenobiotics such as drugs and pesticides (e.g. rotenone). Also, they can be produced by an oxidative-reductive reaction involving  $\text{H}_2\text{O}_2$  and metal ions.<sup>2</sup>

In aerobic systems, oxygen plays a significant role in life processes. Studies show that about five percent of the oxygen inhaled in these systems is converted to ROS by the singlet reduction of oxygen.<sup>3</sup> Also, though mitochondria are the power houses of cells, they are also the site for the majority of ROS production physiologically. In Complex IV of the electron transport chain, a total of four electrons are transferred to oxygen to form two molecules of water; however, electron leakage results in the partial reduction of  $\text{O}_2$  leading to the formation of ROS.<sup>4</sup>

ROS such as  $O_2^{\cdot-}$  and  $H_2O_2$  may be generated from the catalytic activities of cytochromes P450, P450 reductase, and cytochrome *b*-5 reductase in the endoplasmic reticulum. In addition, as a result of tissue injuries, xanthine oxidase is known to produce  $O_2^{\cdot-}$  and  $H_2O_2$  in its catalytic cycle.<sup>5</sup> The most common production of free radicals *in vivo* involves a reaction between transition-metal ions such as copper or iron and  $H_2O_2$ . The Fenton reaction below shows the reduction of  $H_2O_2$  in the presence of  $Fe^{2+}$ .<sup>6</sup>

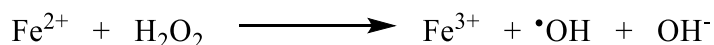


**Figure 1.3:** The reduction of  $H_2O_2$  by  $Fe^{2+}$  to produce the hydroxyl anion and the hydroxyl radical is known as the Fenton reaction.

Another method of producing the hydroxyl radical is the Haber-Weiss reaction. This is a two-step chemical reaction whereby a higher oxidation state metal ion is first reduced by the superoxide anion. This is then coupled with the immediate oxidation of the metal ion and reduction of  $H_2O_2$  resulting in the formation of the hydroxyl anion and the hydroxyl radical (**Figure 1.4**).<sup>7</sup>

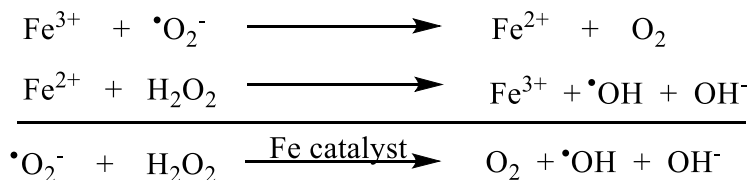


**Figure 1.4:** The Haber-Weiss reaction is a two-step process that begins with the reduction of  $Fe^{3+}$  ion by the superoxide anion coupled with the Fenton reaction which results in the formation of the hydroxyl anion and the hydroxyl radical.

### Antioxidants

When ROS are not controlled they can cause oxidative damage. However, organisms have specialized complexes and enzymes that scavenge ROS and balance the oxidant-antioxidant ratio.<sup>8</sup> Anti-oxidants are mainly free radical scavengers and enzymes

that protect cells from the harmful effects of ROS. The major antioxidant defenses in cells are cytochrome c, superoxide dismutase (SOD), peroxidases, and catalase. Also, there are vitamins and flavoprotein complexes which aid in scavenging ROS.<sup>9</sup> In electron transport, O<sub>2</sub> reduction takes place at the cytochrome a<sub>3</sub>-Cu<sub>B</sub> binuclear complex of complex IV where it binds to oxygen tightly until O<sub>2</sub> is completely reduced to H<sub>2</sub>O.<sup>10</sup>

Superoxide dismutase (SOD) converts the superoxide radical species to hydrogen peroxide and oxygen using two protons and an electron as shown in **Figure 1.5**. SOD the primary antioxidant defense enzyme, is a metalloprotein and located in both prokaryotes and eukaryotes. The SOD found in prokaryotes binds an iron or manganese ion whereas cytosolic SOD in eukaryotes have either bound copper or zinc ion and a bound manganese ion in the isozyme form found in the mitochondrial matrix.<sup>9,10</sup> Although, H<sub>2</sub>O<sub>2</sub> is less toxic in a transition-metal-free system, it may travel beyond its site of generation due to its long-life span and its ability to permeate cell membranes. Catalase reduces hydrogen peroxide to form water. Similar to catalase, peroxidase enzymes such as glutathione peroxidase also reduce hydrogen peroxide by donating hydrogen ions to form water. A cooperative defense system by SOD, glutathione peroxidase, and catalase is shown in **Figure 1.5** below.<sup>10</sup>

In addition to these anti-oxidant enzymes there are ‘scavengers’ which are molecules that react with radicals to produce less harmful radicals. Examples include reduced glutathione (GSH), ascorbate, and α-tocopherol which act cooperatively as cellular antioxidants (**Figure 1.6**). In cell membranes and plasma lipoproteins α-tocopherol functions as a chain-breaking antioxidant to form the tocopherol radical.<sup>11</sup> The tocopherol radical then moves to the membrane surface where it reacts with either ascorbate or GSH to be converted back to α-tocopherol. The ascorbate radical formed can be converted back

to ascorbate by a reduction reaction with GSH which in turn can also scavenge ROS, and the resulting GSSG can be converted back to GSH by reaction with NADPH-glutathione reductase.

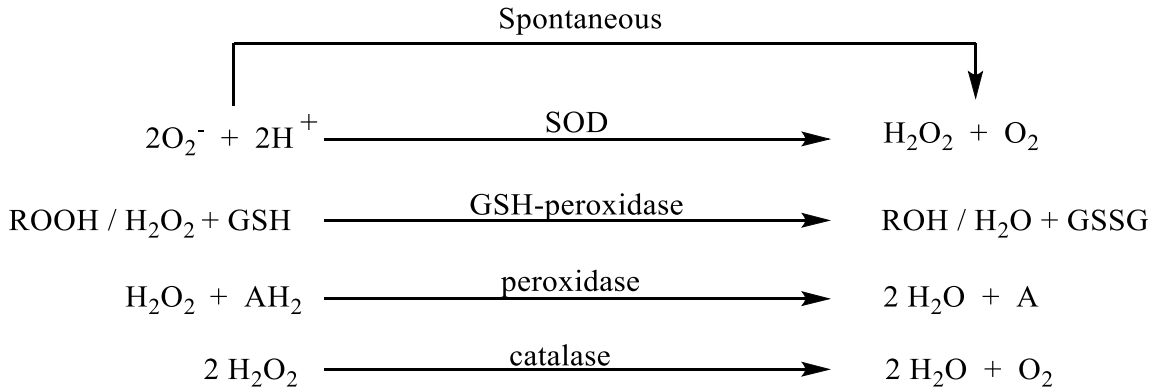


**Figure 1.5.** The neutralization of ROS by antioxidants. Superoxide dismutase (SOD), catalase, and peroxidases form a jointly corporative team of defense against ROS. SOD ensures a steady-state level of superoxide whereas catalase and peroxidases perform a similar function for H<sub>2</sub>O<sub>2</sub>. ROOH represents hydroperoxide and AH<sub>2</sub> is an electron donor.

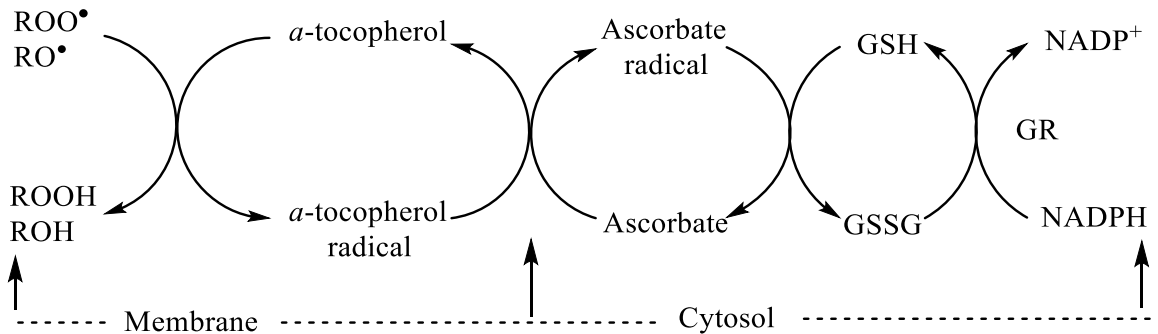


**Figure 1.6:** The “scavengers” α-tocopherol, ascorbate and reduced glutathione (GSH) act as a free radical scavenging mechanism through what is known as the NADPH-glutathione reductase (GR) system with the α-tocopherol reaction occurring in the membrane whereas the ascorbate and reduced glutathione reactions occur in the cytosol.

## Oxidative Damage

ROS can react with cell components such as polyunsaturated fatty acids, proteins, and nucleic acids and cause oxidative damage. This occurs when the production of ROS overwhelms antioxidant defense mechanisms. Oxidative damage results in lipid peroxidation, DNA mutation, protein oxidation, damage to the myelin sheath of the brain, and damage to the mitochondria which eventually leads to apoptosis.<sup>12,13,14</sup> In addition, oxidative damage has been linked to medical conditions such as ischemia, diabetes, cervical cancer, atherosclerosis and many others.<sup>15-19</sup>

The scheme below is a proposed mechanism of ischemia-induced free radical generation leading to tissue damage (**Figure 1.7**). During the catalytic cycle of xanthine oxidase, there is the generation of superoxide ion ( $O_2^{\bullet-}$ ) and  $H_2O_2$ . Xanthine oxidase is produced from the proteolytic cleavage of xanthine dehydrogenase during ischemic conditions. Reperfusion of ischemic tissue provides oxygen which enables xanthine oxidase to act on hypoxanthine or xanthine to produce  $O_2^{\bullet-}$  and  $H_2O_2$  which eventually causes oxidative damage.<sup>14,20</sup>

In cells, transition metal ions such as copper and iron do not exist as redox-active free ions because they are linked to nucleic acids, membranes, proteins or low-molecular weight chelating agents such as histidine, citrate or ATP.<sup>21</sup> There are also specific metal ion carriers that greatly reduce their bioavailability. However, during cellular acidosis and ischemic conditions, transition metal ions are liberated from some metalloproteins which then react with superoxide ion ( $O_2^{\bullet-}$ ) and  $H_2O_2$  to generate the hydroxyl radical.<sup>15</sup>

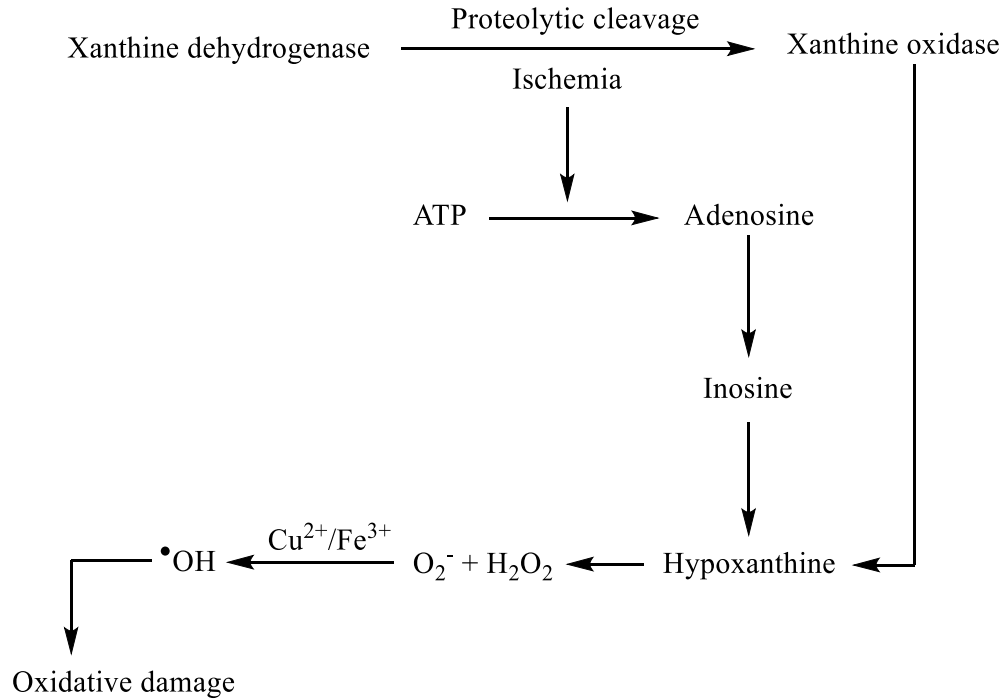


**Figure 1.7:** A scheme showing the presumable cause of ischemia-induced free radical generation and tissue damage.

### Reactive Oxygen Mediated Modification of Proteins

The 20 standard amino acid residues of proteins are all prone to oxidation by the hydroxyl radical ( $\text{OH}\cdot$ ) but oxidized products of some of the residues have not been totally defined. Earlier studies on amino acids and proteins with the superoxide anion and the hydroxyl radical showed that ROS can cause oxidation of amino acids side chains, cleavage of peptide bonds via the  $\alpha$ -amidation or diamide pathway and the generation of covalent protein-protein cross-linked derivatives.<sup>22-28</sup>

**Figure 1.8** shows a possible pathway for the oxidation of the peptide bond. In the scheme, the removal of the hydrogen atom by the hydroxyl radical from the  $\alpha$ -carbon atom initiates a cascade of reactions which results in the formation of water and an alkyl radical (**a**). The addition of an  $\text{O}_2$  molecule to the alkyl radical results in an alkylperoxy radical

(b), which also reacts with a protonated superoxide anion ( $\text{HO}_2^\bullet$ ) or  $\text{Fe}^{2+}$  and  $\text{H}^+$  to form an alkylperoxide (c). The alkylperoxide formed may also react with protonated superoxide anion ( $\text{HO}_2^\bullet$ ) or  $\text{Fe}^{2+}$  and  $\text{H}^+$  to form the alkoxy radical. At this stage, (d), the peptide bond is cleaved or there is further oxidation of the alkoxy radical by the protonated superoxide or  $\text{Fe}^{2+}$  and  $\text{H}^+$  to form a hydroxyl derivative of a peptide. Also, there can be abstraction of hydrogen atoms from amino acid residues by alkoxy, alkyl, peroxy or alkoxy derivatives of peptides to generate new radicals which may also undergo similar modification. At low concentrations or in the absence of  $\text{O}_2$ , there is the formation of intra- and/or interpeptide links from the combination of two alkyl derivatives.<sup>23-28</sup>

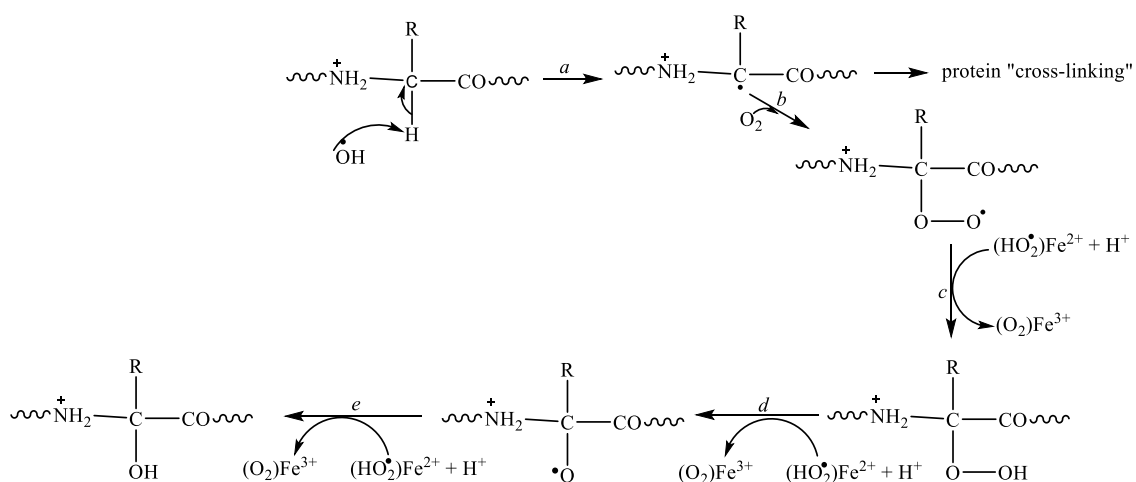


**Figure 1.8:** Possible scheme for the oxidation of the peptide chain.<sup>23-28</sup>

There are at least four possible mechanisms of free radical-induced peptide bond cleavage. These include (1) cleavage of alkoxy derivative peptides via the  $\alpha$ -amidation pathway, (2) cleavage of alkoxy derivative peptides via the diamide pathway, (3) oxidation of side chains of glutamyl and aspartyl residues, and (4) oxidation of the side chains of proline.<sup>23-28</sup>



**Figure 1.9** shows possible mechanisms for both the  $\alpha$ -amidation pathway and the diamide pathway. In the  $\alpha$ -amidation pathway, the product obtained from the N-terminal portion of the amino acid residue of the peptide fragment from the C-terminal portion of the peptide occurs as an isocyanate derivative. The C-terminal product of the peptide formed from the N-terminal portion of the protein is a diamide derivative. In the diamide pathway (**b**), the product obtained from the N-terminal amino acid residue of the peptide fragment as a result of cleavage of the C-terminal portion of the peptide occurs as an  $\alpha$ -ketoacyl derivative whereas the C-terminal amino acid residue of the other peptide occurs as an amide derivative.<sup>29</sup>

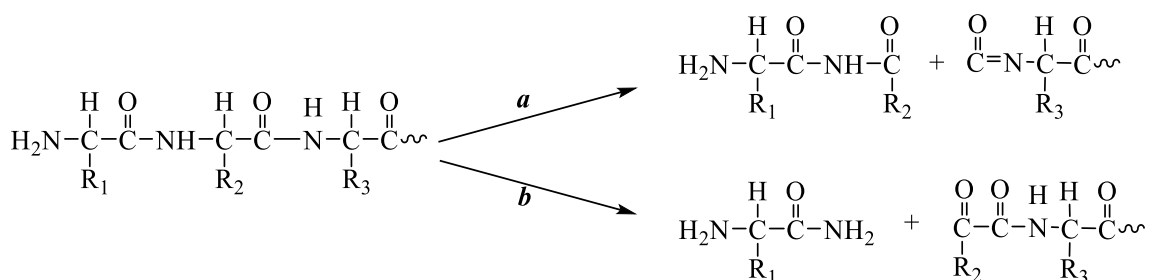


**Figure 1.9:** Possible schemes leading to peptide bond cleavage by the  $\alpha$ -amidation (**a**) or diamide pathway (**b**).<sup>29</sup>

A typical peptide bond cleavage from the attack of a hydroxyl radical on glutamyl residues (**Figure 1.10**) and prolyl residues (**Figure 1.11**) is shown below. The glutamyl residue undergoes a hydroxyl radical attack which leads to peptide bond cleavage where oxalic acid is produced and the N-terminal portion of the amino acid formed from the C-terminal part of the protein occurs as an N-pyruvyl derivative.<sup>30</sup> Likewise, oxidation of the peptide bond at prolyl residues results in the formation of 2-pyrrolidone and its derivatives.<sup>31</sup> In addition, hydrolysis of 2-pyrrolidone results in 4-aminobutyric acid, which is a probable indication of peptide bond cleavage by the proline oxidation pathway.<sup>32</sup>

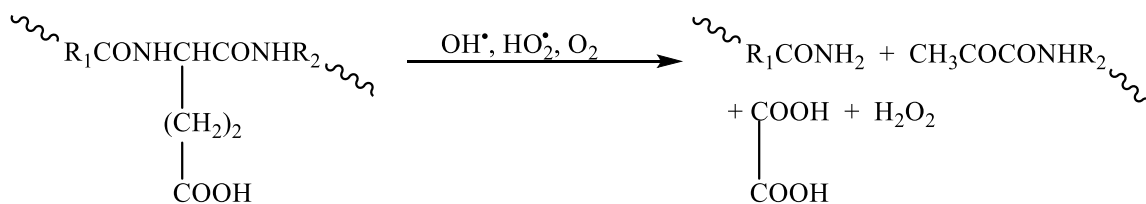


**Figure 1.10:** An OH<sup>•</sup> attack on the side chains of glutamyl residues results in peptide bond cleavage to produce an acetamide, a diacetamide, oxalic acid, and hydrogen peroxide.

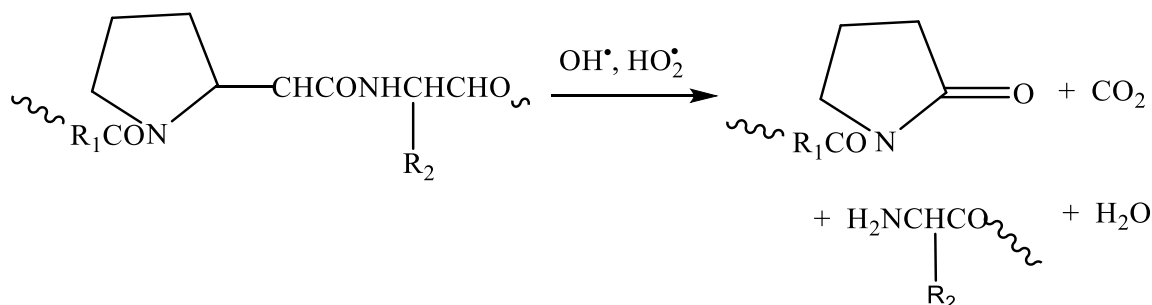


**Figure 1.11:** An OH<sup>•</sup> attack on the side chains of prolyl residues results in peptide bond cleavage.

As discussed previously, the modification of proteins by the  $\alpha$ -amidation pathway or by the oxidation of glutamyl side chains results in the formation of a peptide where the N-terminal amino acid is protected by an  $\alpha$ -ketoacyl derivative. Table 1.1 below shows that oxidation of arginine, lysine, threonine, and proline residues may result in the formation of carbonyl derivatives. Likewise, carbonyl derivatives may be incorporated into proteins by reactions with aldehydes (malondialdehyde, 4-hydroxy-2-nonenal) generated from lipid peroxidation<sup>33-35</sup> or with reactive carbonyl groups (deoxysones, ketoamines, or ketoaldehydes) produced from either reaction of reducing sugars or by the oxidation product of lysine residues of proteins (glycooxidation and glycation reactions).<sup>36-38</sup> Hence, carbonyl groups present in proteins have been used as an indicator of ROS-mediated protein oxidation.<sup>39</sup> The table below illustrates the results of oxidation products for some of the amino acids.<sup>40</sup>

**Table 1.1: Oxidation products of amino acids<sup>27,28</sup>**

Amino Acid	Product
<b>Arginine</b>	Glutamic semialdehyde
<b>Cysteine</b>	CyS-SCy, CyS-SG, CySOH, CySOOH, CySO <sub>2</sub> H
<b>Histidine</b>	2-oxihistidine, 4-OH-glutamate, aspartic acid, asparagine
<b>Leucine</b>	3-OH-leucine, 4-OH-leucine, 5-OH-leucine
<b>Methionine</b>	Methionine sulfoxide, methionine sulfone
<b>Phenylalanine</b>	2-,3- and 4-hydroxyphenylalanine, 2,3-dihydroxyphenylalanine
<b>Tyrosine</b>	3,4-dihydroxyphenylalalnine, Tyr-Tyr cross-links, 3-nitrotyrosine
<b>Tryptophan</b>	2-, 4-, 5-, 6-, and 7-hydroxytryptophan, formylkynurenine, 3-OH-kynurenine, nitrotryptophan
<b>Threonine</b>	2-amino-3-ketobutyric acid
<b>Proline</b>	Glutamylsemialdehyde, 2-pyrrolidone, 4-and 5- OH-proline, pyroglutamic acid
<b>Glutamic Acid</b>	Oxalic acid, pyruvate adducts
<b>Lysine</b>	$\alpha$ -aminoadipylsemialdehyde

### Reactive Oxygen Species in Signal Transduction

Recent studies show that ROS participates in signal transduction. ROS such as the hydroxyl radical, the superoxide ion, and hydrogen peroxide each possesses unique chemical characteristics that impact their signaling function. For instance, among the ROS species, the hydroxyl radical (OH<sup>•</sup>) is the most unstable with a half-life of 10<sup>-9</sup> s and reacts with any molecule within a radius of 30 Å of its site of production, hence, limiting its potential to transmit signals across any distance.<sup>41</sup> The superoxide radical also has limited membrane permeability because it carries a negative charge. On the other hand, H<sub>2</sub>O<sub>2</sub> is

presumed to be capable of permeating due to its neutral nature and reacts with both extra- and intracellular targets giving it a wide reactivity profile.<sup>42</sup> **Figure 1.12.** shows four possible schemes of signal transduction by H<sub>2</sub>O<sub>2</sub>. In the first reaction (*a*) the redox mechanism is based on a scavenging enzyme such as peroxiredoxin (PRX) or glutathione peroxidase (GPX) to transduce the H<sub>2</sub>O<sub>2</sub> with further oxidation of the target protein. The second scheme (*b*), uses the flood gate model, where the scavenger is inactivated by H<sub>2</sub>O<sub>2</sub> either by hyperoxidation to sulfinic acid or posttranslational modification, to enable a hydrogen peroxide mediated oxidation of the target protein. In the third scheme (*c*), the scavenging enzyme becomes oxidized by H<sub>2</sub>O<sub>2</sub> and the oxidized enzyme scavenger oxidizes an intermediate redox protein such as thioredoxin which also further oxidizes the target protein. Finally, in the fourth scheme (*d*), the target protein dissociates from the oxidized scavenging enzyme which results in the activation of the target protein.<sup>43-47</sup>

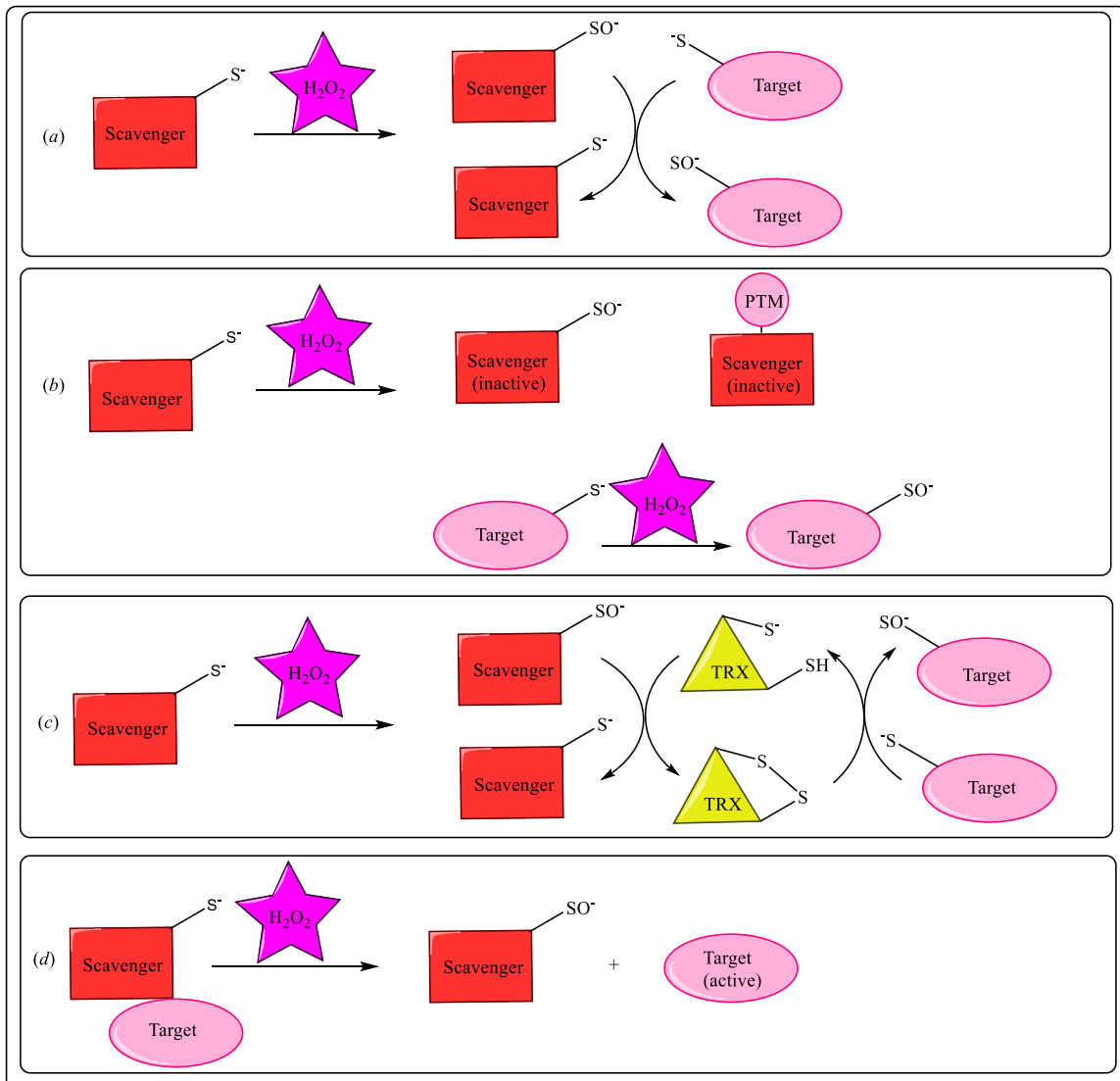


**Figure 1.12:** Possible schemes for  $H_2O_2$ -dependent signal transduction.

### Metal-Catalyzed Oxidation (MCO) Systems

Metal-catalyzed oxidation (MCO) systems are a set of reactions which involves the use of transition metals and  $O_2$  or  $H_2O_2$  to produce ROS. These systems can catalyze the inactivation of enzymes or convert them to less active forms by oxidizing the side chains of the enzymes. In physiological processes, concentrations of  $H_2O_2$  and  $Fe^{3+}$  are a factor in the metal-catalyzed oxidation of proteins. At high concentrations of both  $H_2O_2$  and  $Fe^{3+}$ , it cannot be determined whether the oxidation of proteins is due to MCO. However, low

concentration studies show that the main path for protein oxidation is by MCO systems.<sup>23</sup> Protein oxidation resulting from MCO correlates to the extent of tissue damage and also results in the formation of protein carbonyl derivatives. Below is a list of some MCO systems (**Table 1.2**).

**Table 1.2: Types of MCO Systems**

Non-enzymatic MCO Systems	Enzymatic MCO Systems
Oxygen and Ferric ion	Fe <sup>3+</sup> /O <sub>2</sub> / NADPH oxidase
Oxygen and Ferrous ion	Fe <sup>2+</sup> /O <sub>2</sub> / NADPH oxidase
Ascorbate, Oxygen and Ferrous ion	Fe <sup>3+</sup> /O <sub>2</sub> / Xanthine oxidase
Hydrogen peroxide and Ferrous ion	Fe <sup>3+</sup> /O <sub>2</sub> / Cytochrome P-450 reductase
Ascorbate, Oxygen and Cupric ion	
Hydrogen peroxide and Cupric ion	

A possible mechanism of MCO-mediated protein oxidation is shown in **Figure 1.13**. In the scheme, the ε-amino group of a lysyl residue in the protein is bound to Fe<sup>2+</sup> to form an Fe<sup>2+</sup>-protein coordination complex. Reaction of H<sub>2</sub>O<sub>2</sub> with the Fe<sup>2+</sup>-protein complex results in the formation of OH<sup>-</sup>, OH<sup>•</sup>, and an Fe<sup>3+</sup>-protein complex. Then, the OH<sup>•</sup> radical reacts and abstracts a hydrogen from the carbon bearing the ε-amino group to generate the carbon-centered radical, which also reacts and transfers an unpaired electron to Fe<sup>3+</sup> to reproduce the Fe<sup>2+</sup> protein complex. Simultaneously, the lysyl residue is transformed to an imino derivative, which upon hydrolysis produces ammonia and an aldehyde derivative of the lysyl residue. This results in the destruction of the metal-binding site and the dissociation of Fe<sup>2+</sup> from the protein. This entire process is termed a “caged” reaction if the reaction occurs in a protective pocket of the protein where the ROS produced is protected from radical scavengers.<sup>48,49</sup>

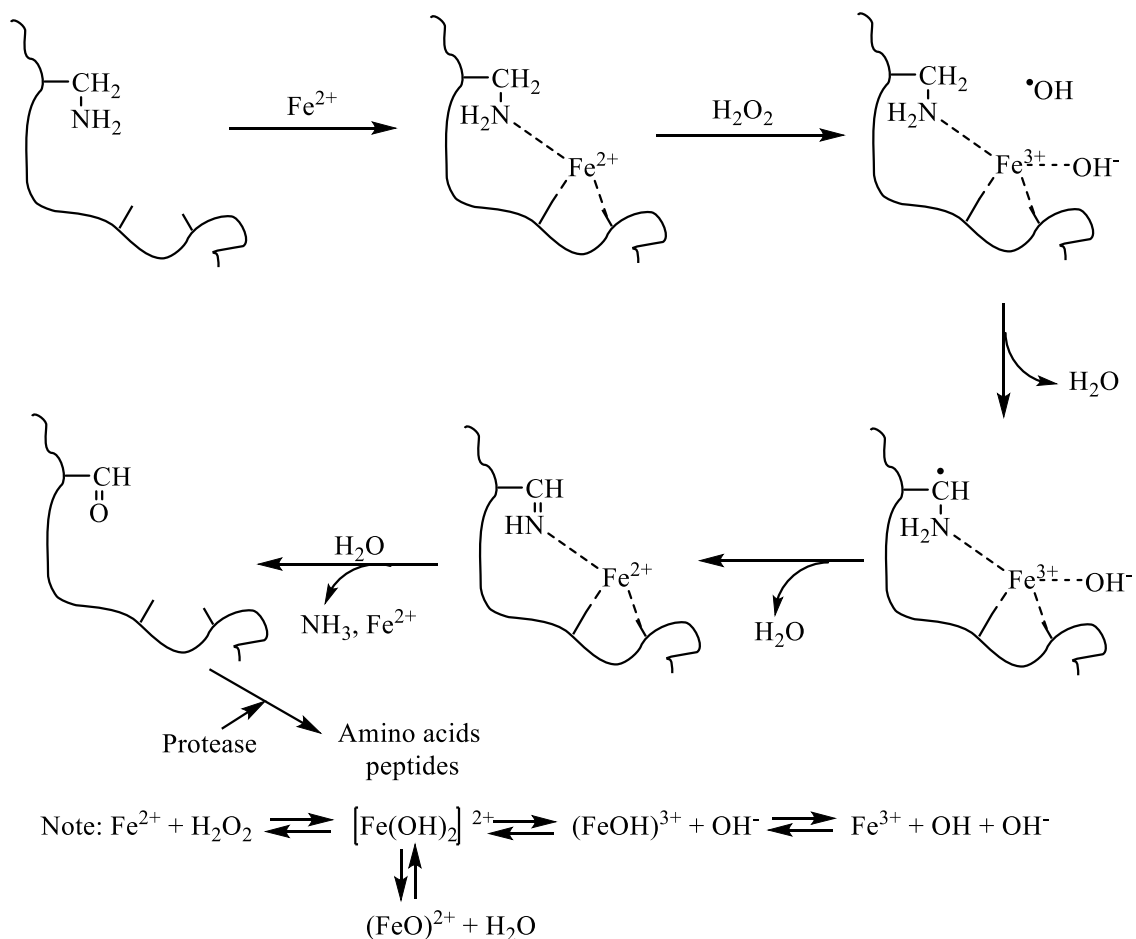


**Figure 1.13:** A possible mechanism for the site-specific metal ion-catalyzed oxidation of proteins by a “caged type” reaction.

### Site Specific Oxidation and Protein Oxidation

Site specific oxidation of proteins is a characteristic of MCO systems. ROS such as the hydroxyl radical produced from MCO reacts immediately with amino acids in the vicinity of its site of production. Amino acids most susceptible to oxidation by MCO systems include Arg, His, Pro, Cys, and Met due to their high affinity for transition metals such as iron and copper.<sup>22,28</sup>

**Figure 1.14** illustrates the oxidation of an amyloid- $\beta$  peptide ( $\text{A}\beta$ ) induced by the ROS generated by the Cu- $\text{A}\beta$ /ascorbate system, in the presence of molecular oxygen. The

hydroxyl radical (HO•) generated by the Fenton-like reaction catalyzed by copper is the most reactive and thus mainly responsible for the oxidation of the Aβ residues. The remaining two ROS produced by the system, hydrogen peroxide and the superoxide anion, also react in some cases with a specific target, for example with methionine residues in peptides and proteins, to produce methionine sulfoxide.<sup>25</sup>

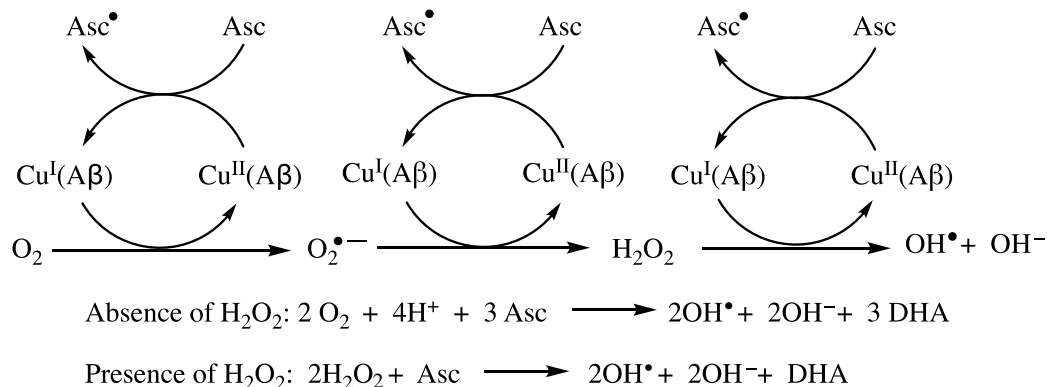


**Figure 1.14:** A site specific oxidation by copper MCO system on amyloid-β peptide (Aβ) in the presence of ascorbate (Asc). In the presence of H<sub>2</sub>O<sub>2</sub>, a three times oxidation of Aβ is achieved compared to the absence of H<sub>2</sub>O<sub>2</sub>. DHA -dehydroascorbate.<sup>25</sup>

High concentrations of oxidized proteins from MCO have been linked to a number of diseases which include Alzheimer's disease, muscular dystrophy, Werner's syndrome, cataractogenesis and rheumatoid arthritis.<sup>28</sup> Also, high concentrations of protein carbonyls have been reported in atherosclerosis, Parkinson's disease, ulcerative colitis, and cystic fibrosis although levels of protein carbonyls have not been directly linked to the cause of these diseases.<sup>8,9</sup>

### Lysozyme

Hen egg white lysozyme (HEWL) is an enzyme made of 129 amino acid residues. HEWL has eight cysteines which construct four disulfide bridges. HEWL's structure is made up of two structural domains: a β-sheet domain and an α-helical domain. Both the α-helical domain and the β-sheet domain have five regions each. The five regions of the α-



helical domain are comprised of three standard  $\alpha$ -helices, with one helix (109-115) similar to the  $\pi$  helix in character while the other two (80-84 and 120-124) are transitional in structure between the  $3_{10}$  helix and the  $\alpha$ -helix. The  $\beta$ -sheet's domain of five regions is comprised of beta sheets, random coils, and beta turns. Furthermore, the interface between the  $\alpha$ -helical domain and the  $\beta$ -sheet domain produces a cleft for substrate binding.<sup>50</sup>

HEWL lyses cells by hydrolyzing the  $\beta$  (1 $\rightarrow$ 4) glycosidic linkages between the N-acetylmuramic acid (NAM) and N-acetylglucosamine (NAG) residues of the cell wall peptidoglycans of bacteria. This is achieved using the two amino acids, Glu35 and Asp52 in the active site.<sup>51</sup> Among the 129 amino acid residues, HEWL has just a single histidyl residue at position 15. The single histidyl residue is found partially buried on the surface of the enzyme and far away from the active site of the enzyme. Also, the histidyl residue has high affinity for copper ions which makes it more susceptible to oxidative modification. According to Madhuri et al., an oxidative change in the histidyl residue causes a slight change in the chemical conformation of the active site but does not affect the optimal activity of the enzyme.<sup>52</sup>

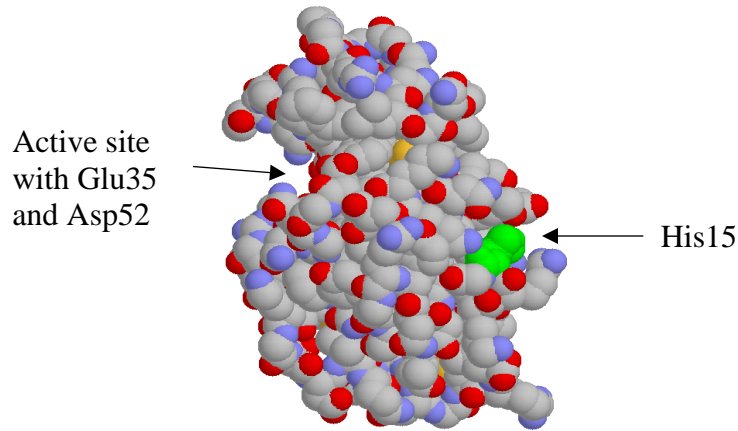


**Figure 1.15:** A picture of HEWL's tertiary structure with His15 in green.

### ***Pichia pastoris* and pPICZ $\alpha$ A<sup>®</sup>.**

*Pichia pastoris* is a methylotrophic yeast strain that can utilize methanol as its only carbon source. It expresses protein intra- or extracellularly at high concentrations when fed with methanol only. *P. pastoris* has the ability to carry out post translational modifications accomplished by higher eukaryotes, which include glycosylation, disulfide bond formation, and proteolytic processing. In addition, it has molecular genetic manipulation mechanisms similar to that of *Saccharomyces cerevisiae*. *P. pastoris*' ability to utilize methanol as a carbon source is due to the activity of alcohol oxidase, *aox* (1 and 2) sequestered in the peroxisome. Finally, *P. pastoris* is economical and easy to manipulate.

pPICZ $\alpha$ A is a plasmid used for methanol-inducible expression of a secreted protein. pPICZ $\alpha$ A contains the alcohol oxidase promoter for the gene, *aox1* and it is responsible for most of the alcohol oxidase activity. It also contains the Zeocin<sup>™</sup> resistance gene as a selective marker. In addition, the  $\alpha$ -factor signal sequence present in pPICZ $\alpha$ A is responsible for the extracellular expression of the gene product. The figure below (**Figure 1.16**), shows pPICZ $\alpha$ A, B and C with the  $\alpha$ -factor and the multiple cloning site.

The pPICZ $\alpha$ A differs from the B and C at the multiple cloning site with the A version having both *Pst* I\* and *Cla* I\* restriction sites. *Pst* I\* is in version B only and *Cla* I\* is in version C only.

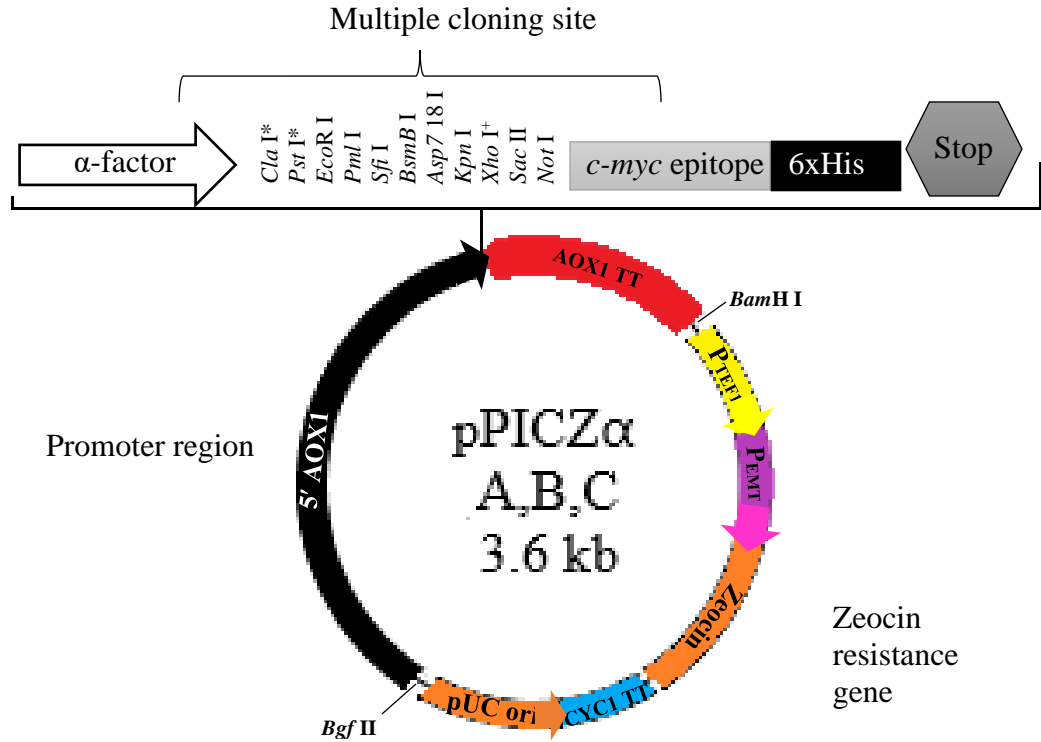


**Figure 1.16:** A picture of the pPICZ $\alpha$  plasmid highlighting the following: the gene that confers Zeocin<sup>TM</sup> resistance, the 5' *aox1* promoter which allows methanol induced high level expression, and the  $\alpha$ -factor signal sequence for extracellular expression.

## RESEARCH STATEMENT

Our research lab has been investigating the metal-catalyzed oxidation of proteins to study the relationship between the level of protein structure and site specific oxidation. The level of protein structure might influence the site of oxidation in one of two ways. The tertiary structure of a protein can create a protective pocket for a “caged” reaction which protects any free radical that is produced from free radical scavengers in the surrounding solution. Alternatively, it is known that certain residues are more susceptible to metal

catalyzed oxidation due to their ability to chelate metal ions. Perhaps all that is important is for the presence of these metal chelating residues in the primary sequence.

The model protein for our research is hen egg white lysozyme (HEWL). Different mutant forms of HEWL have been developed for the investigation of oxidative modification of proteins by ROS. HEWL H15S, a mutant of HEWL where the histidine in position 15 was substituted with serine, has been cloned into *P. pastoris*. This residue substitution of histidine at position 15 removes the metal chelating property at that position. This research is focused on examining the growth parameters for the *P. pastoris* X-33-pPICZ $\alpha$ A-*hewl*H15S strain to optimize the small scale expression of HEWL H15S.

## CHAPTER 2: MATERIALS AND METHODS

### Materials and Instruments

Yeast nitrogen base (YNB), ammonium sulfate, peptone, protein loading dye, glycerol, AGAR, bacteriological yeast extract, Blue BANDit™ Protein Stain and casamino acid were obtained from Amresco (Framingham, MA). Biotin, *Micrococcus lysodeiktitus*, antifoam 204 and 2-(N-morpholino) ethanesulfonic acid (MES) were obtained from Sigma Aldrich (St. Louis, MO). EDTA (disodium salt), dextrose, potassium phosphate and HPLC grade methanol were obtained from Fisher Scientific (Fair Lawn, NJ). Zeocin™ was obtained from Invitrogen. Bovine serum albumin (BSA), Coomassie brilliant Blue dye R-250, Precision Plus Protein™ Dual Color protein marker and Mini-PROTEAN® TGX™ SDS-PAGE gels and 10× Tris/Glycine/SDS were obtained from Bio-Rad (Hercules, CA). Glass beads, 0.5 mm diameter were obtained from Biospec Products, Inc. (Bartlesville, OK). Antifoam A concentrate from Sigma Aldrich (Saint Louis, MO).

Instruments used for the experiment included a Mettler AE100 balance (Columbus, OH), an Agilent 8453 UV-Vis spectrophotometer (Santa Clara, CA) with the Chemstation software suite by Hewlett Packard, a double pan balance for balancing before centrifuging (American Scientific Products, Columbus, OH), a heat block (VWR Scientific, Radnor, PA), a maxi mix II vortex (Thermolyne, Waltham, MA), a Tuttnauer 3850M autoclave (Heidolph-Brinkman, Schwabach, Germany), a high speed Avanti™ J-25I Centrifuge (Beckman Coulter, Indianapolis, IN), a table top Sorvall® RT 6000B Refrigerated Centrifuge (Mundelein, IL), a table top Fisher Scientific accuSpin™ Micro centrifuge (Waltham, MA), shaker water bath (New Brunswick Scientific, Edison, NJ), Orbital shaker

(purchased from Cole Parmer, Vernon Hills, IL) and Accumet Digital pH meter from Fischer Scientific (Fair Lawn, NJ).

## **Method**

The procedure used for the small scale expression was based on the EasySelect™ *Pichia* Expression Kit, Version G, manual for expression of recombinant proteins using the pPICZ and pPICZα plasmids for *Pichia pastoris*.

### ***Preparation of YPD Plates***

For a 100 mL solution, yeast extract (1% (w/v)), peptone (2% (w/v)) and agar (2% (w/v)) were dissolved in 90 mL of water and the solution was autoclaved for 20 min on the liquid cycle. After autoclaving, the solution was allowed to cool to about 60 °C and 10 mL of 10X D (10% (w/v) dextrose) and 100 μL of 100 mg/mL Zeocin™ were added. About 15 mL of the solution was then poured into each of six separate petri dish plates. The media was stable for one to two weeks at 4 °C.

### ***Buffered Glycerol-complex Medium (BMGY)***

For 100 mL solution, yeast extract (1% (w/v)) and peptone (2% (w/v)) were dissolved in 70 mL of water and the solution was autoclaved on the liquid cycle for 20 min. The solution was allowed to cool to room temperature and the following were added and mixed well: 10 mL 1M MES, pH 5.5, 10 mL 10X YNB (13.4% yeast nitrogen base with 1% (w/v) (NH<sub>4</sub>)<sub>2</sub>SO<sub>4</sub>, 200 μL 500X B (0.02% (w/v) biotin) and 10 mL 10X GY (10% (v/v) glycerol). The solution is sterile and is stable for about 2 months when stored at 4 °C.

### ***Buffered Methanol-complex Medium (BMMY) + 1% casamino acids + EDTA***

For a 500 mL solution, yeast extract (1% (w/v)), casamino acid (1% (w/v)) and peptone (2% (w/v)) were dissolved in 340 mL of water and the solution was autoclaved on the liquid cycle for 20 min. The solution was allowed to cool to room temperature and the following were added and mixed well: 50 mL 1M MES, pH 5.5, 50 mL 10X YNB, 1 mL 500X B, 50 mL 10X M and 5 mL of 100 mM EDTA. The solution is sterile and stable for about 2 months when stored at 4 °C.

### ***Growth of Yeast Strains***

*Pichia pastoris* yeast strain X-33, containing the pPICZ $\alpha$ A recombinant plasmid with the gene (*hew/H15S*), was previously prepared by Nichole Patton and Dr. Michael Serra (YSU). Yeast from a frozen stock solution was streaked on the YPD plates and allowed to grow for about 72 hours at room temperature.

### ***Small Scale Expression of Hen Egg White Lysozyme Mutant (HEWL H15S)***

For the general procedure of expression, a single colony of the *P. pastoris* X33-pPICZ $\alpha$ A-*hew/H15S* strain was used to inoculate BMGY media (25 mL) in a 250 mL baffled flask. The yeast was allowed to grow at 28-30 °C with shaking at 250-300 rpm until the culture reached an OD<sub>600</sub> of 2.

The cells were harvested by centrifugation at 3,000  $\times$  g for 5 minutes at room temperature. The supernatant was decanted and the tubes inverted on a paper towel to drain the glycerol containing buffer. The pellet was resuspended in BMMY + EDTA + 1% casamino acids (BMMY + E + 1% caa) media at room temperature and centrifuged for 5 min at 3,000  $\times$  g. The supernatant was decanted, and the pellet was resuspended once again in BMMY + E + 1% caa.

The suspended cells (from 0.2-1 mL) were pipetted and added to approximately 95 mL BMMY + E + 1% caa. Enough suspended cells were added to achieve an OD<sub>600</sub> of about 1.

The cell suspension was transferred into a 1 L baffled flask and the flask was covered with 2 layers of sterile cheese cloth. The culture was allowed to grow at 28-30 °C with shaking at 250 rpm. Methanol was added to a final concentration of 0.5% (v/v) every 24 hs to maintain induction.

At 24 hour intervals, a 1 mL aliquot of the culture was removed, transferred into a 1.5 mL microcentrifuge tube, centrifuged at  $3,000 \times g$  to separate the cells from the supernatant and both pellet and supernatant were stored in a -80 °C freezer until ready for analysis. After 96 hours, the culture was centrifuged at  $3,000 \times g$  to harvest the cells for 2-3 minutes at room temperature. The pellet was frozen in a dry ice bath before being stored in the -80 °C freezer and the supernatant also saved at -80 °C for analysis of expressed protein.

#### ***Ammonium Sulfate Fractionation***

Ammonium sulfate fractionation was performed on the supernatant to precipitate out proteins. First, the supernatant was taken to 65% ammonium sulfate saturation with stirring for 30 min at 4 °C. The saturated solution was centrifuged at  $16,000 \times g$  for 30 min. The pellet was resuspended in about 2 mL of 0.1 M potassium phosphate buffer (KP<sub>i</sub>), pH 7. The remaining solution was taken to 85% ammonium sulfate saturation at 4 °C with stirring. The solution was then centrifuged at  $16,000 \times g$  for 30 min. The pellet was suspended in about 2 mL of 0.1 M KP<sub>i</sub>, pH 7. The 65% and 85% suspensions were dialyzed separately against 0.1 M KP<sub>i</sub>, pH 7.



### ***Bradford Assay***

A Bradford assay was performed to determine the protein concentration of the collected samples. A blank (100  $\mu$ L of BMMY) and 4 standards of BSA (10, 30, 50, and 70  $\mu$ g) were prepared using 3 mL of Bradford reagent in each solution. The samples were allowed to incubate at room temperature for 10 minutes and their absorbance was measured at 595 nm. A standard curve was then generated.

Samples under study were prepared by mixing 50  $\mu$ L of sample and 50  $\mu$ L of water with 3 mL of Bradford reagent. After incubating at room temperature for 10 minutes their absorbance was measured at 595 nm. The protein concentration was determined from the standard curve.

### ***SDS-PAGE***

A 50  $\mu$ L aliquot of each sample was mixed with 50  $\mu$ L of the 2x protein loading dye. Each mixture was heated in a heat block at 100  $^{\circ}$ C for 4 min and allowed to cool to room temperature. The samples (20  $\mu$ L each) were loaded into each well of the 8 – 16% polyacrylamide gel. A 10  $\mu$ L sample of the Precision Plus Protein Standards was loaded into one of the lanes as well. The gel was electrophoresed at 170 V for about an hour using a running buffer with 0.1% SDS. The resulting gel was developed with Blue-BANDit<sup>TM</sup> to detect the bands of protein.

### ***Gel Staining for Protein Detection***

Blue-BANDit<sup>TM</sup> was used to detect proteins in the gels. The procedure was done in a three step process which included a pre-wash, a staining and a destaining step. During the pre-wash, the gel was placed in a Tupperware container and covered with about 100 mL of deionized water. The gel was microwaved for one minute, allowed to sit for a minute

and the water was discarded. This was repeated two more times. In the staining process, the water was poured out of the container and about 40 mL of Blue-BANDit™ was added. The gel was microwaved for a minute and allowed to sit on the shaker with gentle shaking for about 30 min. In the final step, which is destaining, the stain solution was poured off and 100 mL of water was added to the container. The set up was allowed to sit on a shaker with gentle shaking until protein bands were visible.

### ***Enzyme Assay***

The rate of lysis of *Micrococcus lysodeikticus* was determined based on the approach suggested by Shugar (1952).<sup>55</sup> A unit is equivalent to a decrease in turbidity of 0.001 per minute at 450 nm at pH 7.0 and 25 °C under the specified conditions.

A 0.3 mg/mL suspension of *Micrococcus lysodeikticus* cells in 0.1 M potassium phosphate, pH 7 was prepared and stored in the refrigerator at approximately +4 °C for at least 24 hours to ensure full suspension of the cells.

A lysozyme standard was assayed with the samples due to the difference in cell substrate. Native lysozyme was dissolved to a concentration of 1 mg/mL in cold DI water. Since the protein may contain some salt contaminants, the absorbance of solution was measured at 280 nm to determine the protein concentration using **Equation 2-I** below.

$$\% \text{ protein} = A_{280} \times 0.39 \times 100 \quad \text{(Equation 2-I)}$$

where 0.39 is a protein concentration correction factor for salt impurities. The lysozyme solution was then kept on ice until it was time to perform the assay. After the first assay, the enzyme solution was further quantitatively diluted in cold water to achieve a rate between 0.015 – 0.040  $\Delta A_{450}$ /minute.

For the assay, the spectrophotometer was set to 450 nm. A circulating water bath was installed to maintain a temperature of 25 °C. The absorbance of the suspension of the native enzyme and the samples were measured every 10 sec for a total of 240 sec using the kinetic assay mode on the Agilent diode array spectrophotometer. The zero-order option was selected and the rate was multiplied by negative 60 to give a corrected rate of  $\Delta A_{450}/\text{minute}$ .

To achieve a blank rate, 2.9 mL of the *Micrococcus lysodeikticus* cell suspension was pipetted into the cuvette and incubated for 4-5 min to achieve temperature equilibration before measuring. In the case of the native enzyme and diluted samples, 0.1 mL of each solution was added to a 2.9 ml of *Micrococcus lysodeikticus* cell suspension in the cuvette after equilibration. Three measurements of were made for each assay The  $\Delta A_{450}/\text{minute}$  for each solution was determined by subtracting the average absorption rate of the blank from the absorption rate of the individual samples measured. Equation 2-II was used to determine the activity in units/mg.

$$\text{Units/mg} = (\Delta A_{450}/\text{minute} \times 1000) / (\text{mg enzyme in reaction mix}) \quad \text{(Equation 2-II)}$$

$$\text{mg enzyme in reaction mix} = \text{mg/mL} \times \text{mL of aliquot, i.e. 0.100 mL} \quad \text{(Equation 2-III)}$$

### ***Analysis of Intracellular Protein Expression by SDS-PAGE***

After the 1 mL aliquots were collected at 24 h intervals from growth in 0.5% (v/v) GY with different EDTA, CaCl<sub>2</sub> and MeOH concentrations the cells were lysed using Breaking Buffer and acid-washed 0.5 mm diameter glass beads. For a liter of 50 mM Breaking Buffer, 6.0 g sodium phosphate (monobasic), 372 mg EDTA and 50 mL glycerol was added to 900 mL deionized water and the pH adjusted to 7.4 using NaOH. The solution volume was then brought to one liter using a volumetric flask. A 1 mM phenylmethyl

sulfonyl fluoride (PMSF) solution was prepared using isopropanol as solvent and used as the protease inhibitor.

The cell pellets from the 1 mL aliquots stored every 24 hours were thawed quickly and placed on ice. For each 1 mL sample, 100  $\mu$ L of Breaking Buffer and 30  $\mu$ L of 1 mM PMSF were added to suspend the cell pellet. An equal volume of acid-washed glass beads was added and the mixture was vortexed for 30 seconds and then incubated on ice for 30 seconds. This was repeated for a total of 8 cycles. The resulting mixture was centrifuged at 14,000 rpm at 4 °C for 10 minutes and the clear supernatant transferred into a clean microcentrifuge tube. To 20  $\mu$ L of supernatant cell lysate, 20  $\mu$ L of 0.125 M Breaking Buffer (achieved by 1:3 dilution of Breaking Buffer with DI H<sub>2</sub>O), 10  $\mu$ L of 10% SDS and 6  $\mu$ L of  $\beta$ -mercaptoethanol were added and the mixture was boiled for 5 minutes. After the mixture cooled to room temperature, equal volumes (56  $\mu$ L) of 20% glycerol and 10  $\mu$ L of bromophenol blue were added and the solution was centrifuged. About 20  $\mu$ L of the resulting solution was loaded on the gel for analysis as previously described above.

### ***Optimization of Pichia pastoris Protein Expression***

*P. pastoris* X33-pPICZ $\alpha$ A-*hewl*H15S initially grown on YPD plates as previously described was inoculated into two different glycerol concentrations (0.5% (v/v) and 1% (v/v)) of BMMY. Growth curves were generated over time for the two different conditions by taking 1 mL samples every 3 hours and measuring an absorbance at 600 nm of a 10-fold diluted sample until the absorbance had plateaued. This was performed to determine the midpoint of the growth curve.

The methanol concentration in BMMY medium was altered to determine its effect on protein expression. Three different concentrations were investigated: 0.5% (v/v), 1%

(v/v) and 2% (v/v) MeOH. In addition, yeast was grown at either 28 °C or 22 °C to investigate the effect of temperature on cell growth and protein expression. The supernatant fractions and/or cells grown under each methanol and temperature condition were then analyzed for protein concentration by SDS-PAGE and for enzyme activity as described previously.

Finally, effects of addition of CaCl<sub>2</sub> and the elimination of EDTA on protein expression were also examined. Three different conditions were set up for investigation: BMMY + 1% caa + CaCl<sub>2</sub> – EDTA at 0.5% (v/v) MeOH, BMMY + 1% caa + CaCl<sub>2</sub> – EDTA at 1% (v/v) MeOH and BMMY + 1% caa+ CaCl<sub>2</sub> + EDTA at 0.5% (v/v) MeOH. The supernatant fractions and/or cells grown under each condition were analyzed for protein concentration by SDS-PAGE and for enzyme activity as described previously.

Intracellular expression was analyzed by lysing the cells using Breaking Buffer and acid-washed glass beads as described previously. The supernatant of the lysed cells after centrifugation was analyzed for protein concentration by SDS-PAGE and for enzyme activity as described previously.

## CHAPTER 3: RESULTS

Previous work on the small scale expression of HEWL H15S has not shown significant expression of the mutant enzyme. Different growth conditions for *P. pastoris* X33-pPICZ $\alpha$ A-*hewl*H15S were examined as well as different conditions to optimize the extracellular expression of protein. Intracellular expression of the protein was also examined to determine the distribution of the H15S mutant.

### *The Effect of pH on the Growth of P. pastoris X33-pPICZ $\alpha$ A-hewlH15S*

Both BMGY and BMMY were prepared and their pH was adjusted to 5.0. Using the procedure for small scale expression, a single colony of *P. pastoris* X33-pPICZ $\alpha$ A-*hewl*H15S was grown on a YPD plate for 3 days and transferred into 25 mL of BMGY in a 100 mL baffled flask. The flask was secured to a shaking water bath set to 250 rpm and a temperature of 29.8 °C for 24 hours. The results are shown in **Table 3.1** below.

**Table 3.1:** Optical density at 600 nm of yeast culture grown in BMGY, pH 5.0

Buffered Medium	Time (Hs)	OD <sub>600</sub>
BMGY	16	0.12
BMGY	24	0.18

### *The Effect of Methanol Concentration on the Extracellular Expression of HEWL H15S*

The *P. pastoris* X33-pPICZ $\alpha$ A-*hewl*H15S was grown in BMMY media with either 0.5% (v/v) or 1% (v/v) methanol to examine the effect of methanol concentration on H15S expression. Both the BMGY and BMMY media were buffered at a pH of 5.5. The yeast was grown in a shaking water bath set to 250 rpm and a temperature of 30 °C. One mL aliquots of the media were collected every 24 hs from 24 to 96 hs. A Bradford assay was performed on supernatant to determine the amount of protein secreted. SDS-PAGE was

performed to examine protein expression with time. Finally, the enzyme activity of each supernatant fraction was determined using a suspension of *Micrococcus lysodeikticus* cells in phosphate buffer at pH 7.0.

### **Bradford Assay**

A standard curve was generated using bovine serum albumin (BSA) as a standard to determine the concentration of proteins in the media from the collected samples. One mL fractions obtained at 24, 48, 72, and 96 h were analyzed. In addition, the concentrated and dialyzed 96 h sample obtained from an 85% ammonium sulfate saturation cut of approximately 90 mL of media was assayed. The plot of absorbance at 595 nm vs  $\mu\text{g}$  of BSA to generate a standard curve and determine the protein concentration of each fraction is shown in **Figure 3.1** below.

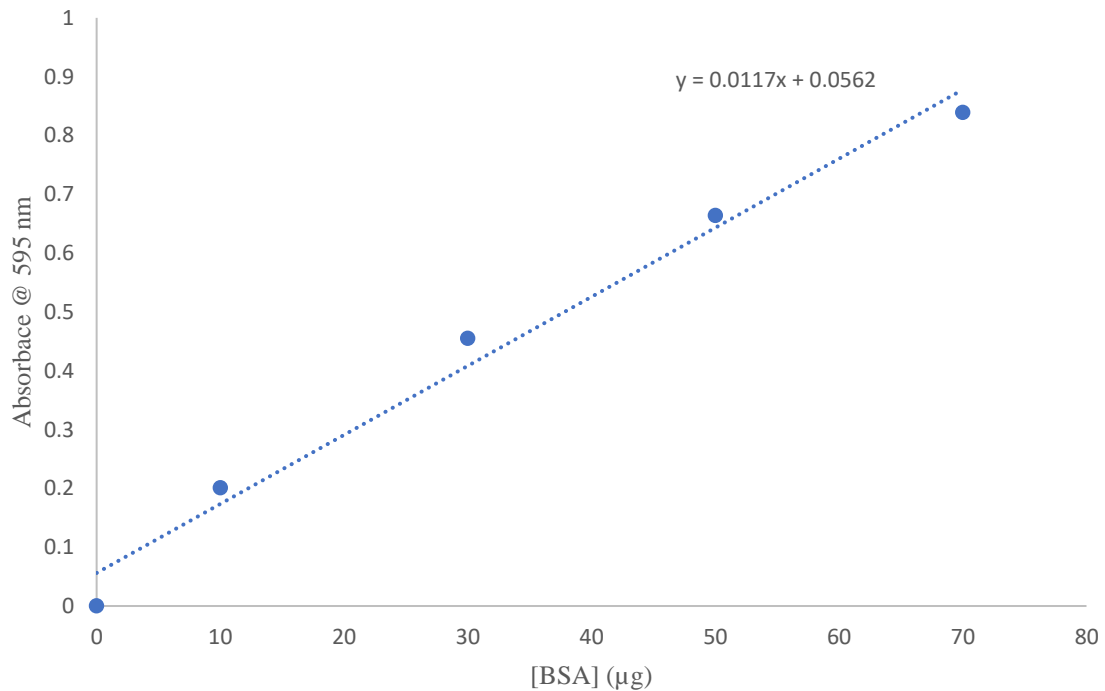


**Figure 3.1:** A plot of absorbance at 595 nm vs  $\mu\text{g}$  of BSA.

**Table 3.2:** Bradford Assay of supernatant fractions grown in either 0.5% (v/v) or 1% MeOH collected at 24 h intervals from 24 to 96 hours.

Sample (50 $\mu$ L)	[(NH <sub>4</sub> ) <sub>2</sub> SO <sub>4</sub> ] (%)	[MeOH] (%)	Time (Hs)	Absorbance @ 595 nm	[Protein] (mg/mL)
<b>BSA (10 <math>\mu</math>g)</b>				0.201	
<b>BSA (30 <math>\mu</math>g)</b>				0.455	
<b>BSA (50 <math>\mu</math>g)</b>				0.664	
<b>BSA (70 <math>\mu</math>g)</b>				0.839	
<b>T.3.2:1A</b>		0.5	24	0.091	0.059
<b>T.3.2:1B</b>		0.5	48	0.125	0.118
<b>T.3.2:1C</b>		0.5	72	0.200	0.246
<b>T.3.2:1D</b>		0.5	96	0.314	0.441
<b>Precipitated T.3.2:1D</b>	85	0.5	96	0.377	0.548
<b>T.3.2:2A</b>		1	24	0.087	0.053
<b>T.3.2:2B</b>		1	48	0.091	0.059
<b>T.3.2:2C</b>		1	72	0.110	0.092
<b>T.3.2:2D</b>		1	96	0.144	0.151
<b>Precipitated T.3.2:2D</b>	85	1	96	0.303	0.423

An SDS-PAGE of the supernatant fractions of expressed protein grown in 0.5% (v/v) MeOH at different time points was performed and the results are shown in **Figure 3.2A**.



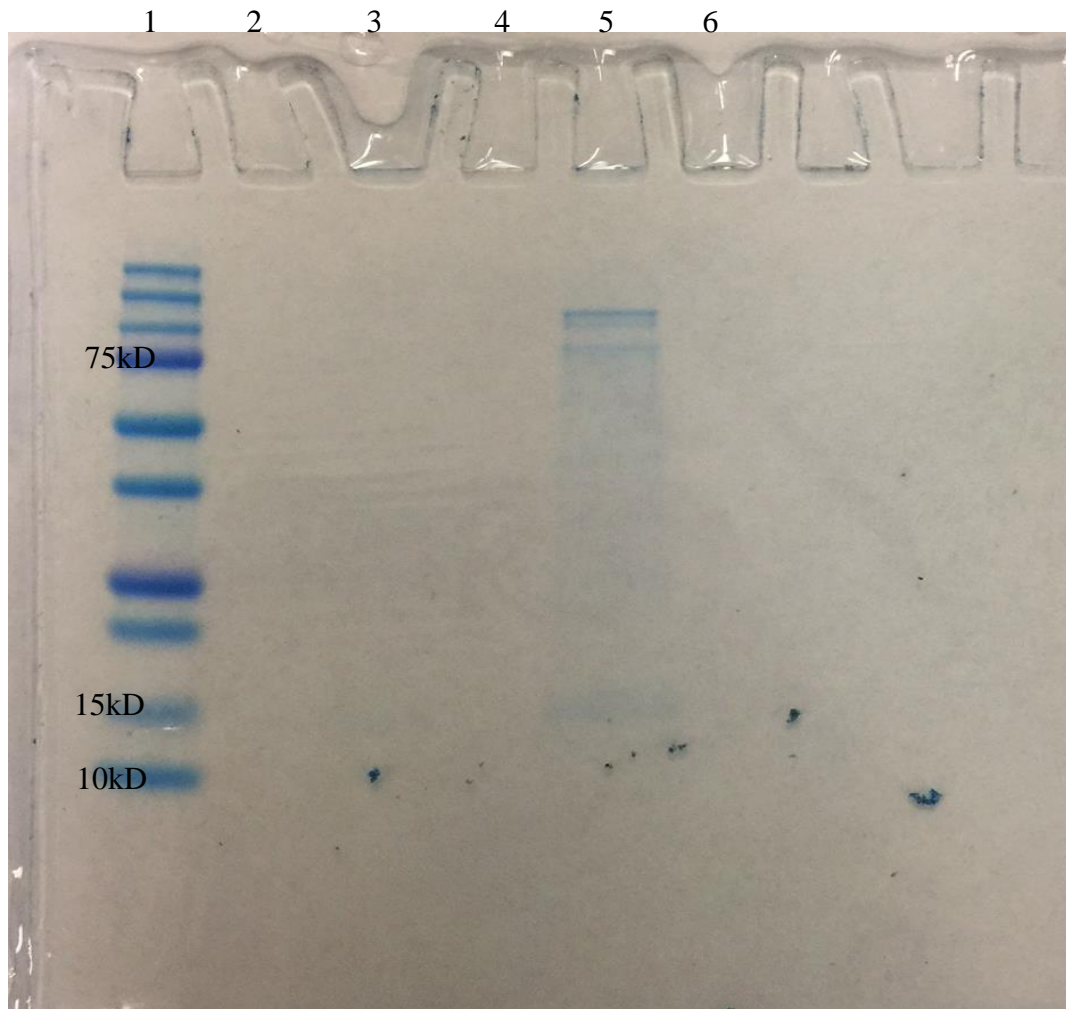


**Figure 3.2A:** SDS-PAGE of supernatant samples from *P. pastoris* X33-pPICZαA-*hewlH15S* grown in BMMY with 0.5% (v/v) methanol. Samples were analyzed using a Mini-PROTEAN TGX™ 8-16% ready-made gel from Bio-Rad. Lane 1 corresponds to the Precision Plus Protein Standards from Bio-Rad, Lanes 2, 3, 4 and 6 corresponds to 24, 48, 72 and 96 h time point samples respectively and Lane 5 corresponds to the concentrated and dialyzed 85% ammonium sulfate cut at 96 h.

An SDS-PAGE of the supernatant fractions of expressed protein grown in 1% (v/v) MeOH at different time points was performed and the results are shown in **Figure 3.2B**.

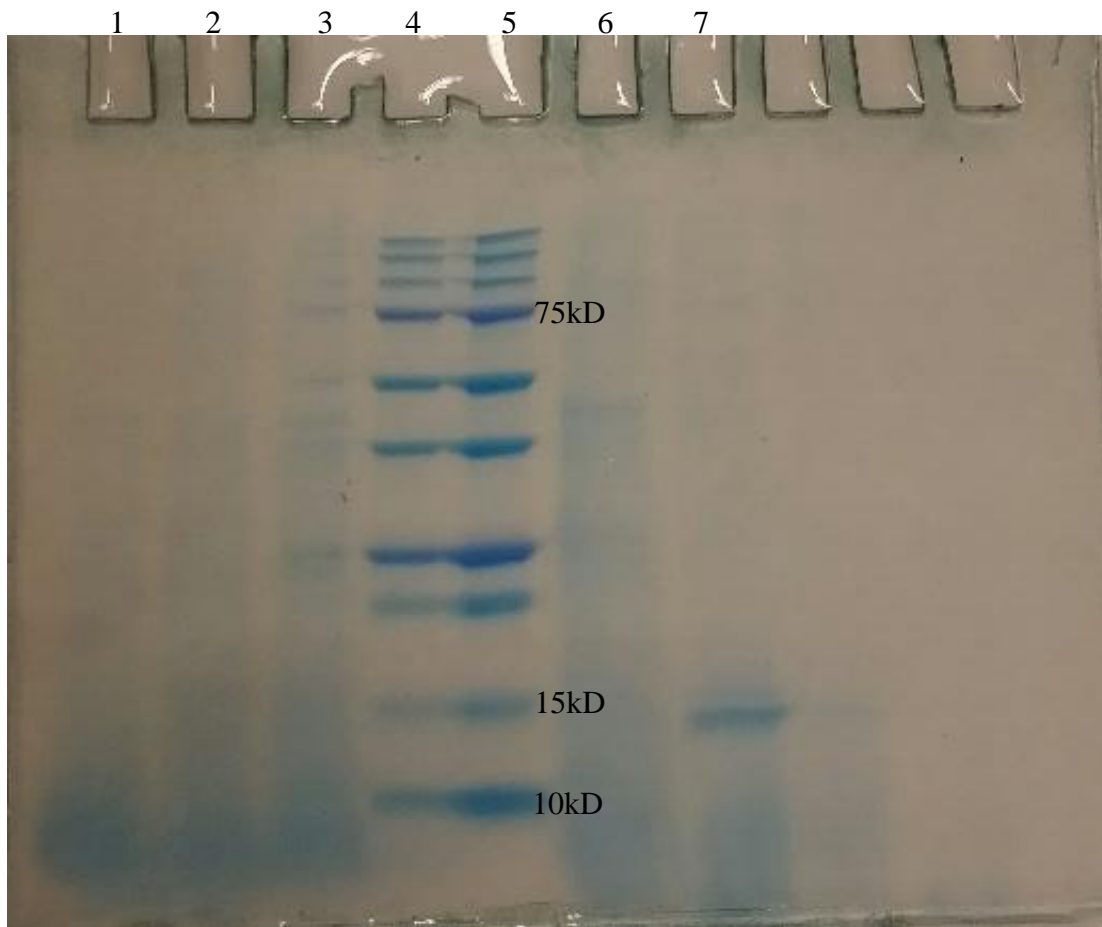


**Figure 3.2B:** SDS-PAGE of supernatant samples from *P. pastoris* X33-pPICZαA-*hewl*H15S grown in BMMY with 1% (v/v) methanol. Samples were analyzed using a Mini-PROTEAN® TGX™ 8-16% ready-made gel from Bio-Rad. Lanes 1, 2, and 3 corresponds to 24, 48 and 72 h time point samples respectively. Lane 4 and 5 corresponds to the Precision Plus Protein Standards from Bio-Rad, Lane 6 corresponds to 96 h time point sample and Lane 7 corresponds to the concentrated and dialyzed 96 h 85% ammonium sulfate cut.

### ***Enzyme Assay***

Enzyme assays were conducted on the supernatant fractions collected from growth in BMMY media at both the 0.5% (v/v) and 1% (v/v) methanol concentrations using a suspension of *Micrococcus lysodeikticus* cells in potassium phosphate buffer at pH 7.0. The activity of the samples was compared to that of the native HEWL enzyme and the results are shown in **Table 3.3** below.

**Table 3.3:** Determination of enzyme activity of samples grown in either 0.5% (v/v) or 1% (v/v) MeOH collected at 24 h intervals from 24 to 96 hs.

Sample (100 µl)	[(NH <sub>4</sub> ) <sub>2</sub> SO <sub>4</sub> ] (%)	[MeOH] (%)	ΔA/ min @ 450 nm	Time (Hs)	Units/mg
<b>Blank</b>			0		
<b>*Native HEWL</b>			0.019		2.38 × 10 <sup>6</sup>
<b>T.3.2:1A</b>		0.5		24	†nd
<b>T.3.2:1B</b>		0.5		48	nd
<b>T.3.2:1C</b>		0.5		72	nd
<b>T.3.2:1D</b>		0.5		96	nd
<b>Precipitated T.3.2:1D</b>	85	0.5	0.022	96	395
<b>T.3.2:2A</b>		1		24	nd
<b>T.3.2:2B</b>		1		48	nd
<b>T.3.2:2C</b>		1		72	nd
<b>T.3.2:2D</b>		1		96	nd
<b>Precipitated T.3.2:2D</b>	85	1	0.046	96	1092

\*The native enzyme was diluted 100-fold for the enzyme assay.

†Enzyme activity was not detected.

### ***Growth at 28 °C and Protein Precipitation at Different Ammonium Sulfate Concentrations***

Small scale expression of the H15S lysozyme protein was performed at 28 °C with shaking at 250 rpm. *P. pastoris* X33-pPICZαA-hewlH15S were grown in BMMY buffered at pH 5.5 at different MeOH concentration of 0.5% (v/v) and 1% (v/v). The protein was precipitated from both media in two steps. First the media was made 65% in (NH<sub>4</sub>)<sub>2</sub>SO<sub>4</sub>. The 65% solutions were then raised to 85% (NH<sub>4</sub>)<sub>2</sub>SO<sub>4</sub>. The Bradford assay, SDS-PAGE and an enzyme activity assay using a suspension of *Micrococcus lysodeikticus* cells in phosphate buffer at pH 7.0 were performed to analyze protein expression at 96 h.

**Table 3.4:** Bradford Assay of the 96 h growth fractions initially grown in either 0.5% (v/v) or 1% (v/v) MeOH. The protein was precipitated at 65% (NH<sub>4</sub>)<sub>2</sub>SO<sub>4</sub> or between 65 – 85% (NH<sub>4</sub>)<sub>2</sub>SO<sub>4</sub>

Sample (50 µL)	[MeOH] (%)	(NH <sub>4</sub> ) <sub>2</sub> SO <sub>4</sub> Cut (%)	Absorbance @ 595 nm	[Protein] (mg/mL)
BSA(10 µg)			0.281	
BSA(30 µg)			0.666	
BSA(50 µg)			1.007	
BSA(70 µg)			1.266	
T.3.4:1	0.5	65	0.714	0.688
T.3.4:2	0.5	65 – 85	0.769	0.754
T.3.4:3	1	65	0.534	0.465
T.3.4:4	1	65 – 85	0.850	0.852

The SDS-PAGE of the 96 h samples from yeast grown at 28 °C is shown in **Figure 3.3**. Protein was expressed with either 0.5% (v/v) or 1% (v/v) MeOH. Protein was precipitated using two different (NH<sub>4</sub>)<sub>2</sub>SO<sub>4</sub> cuts.

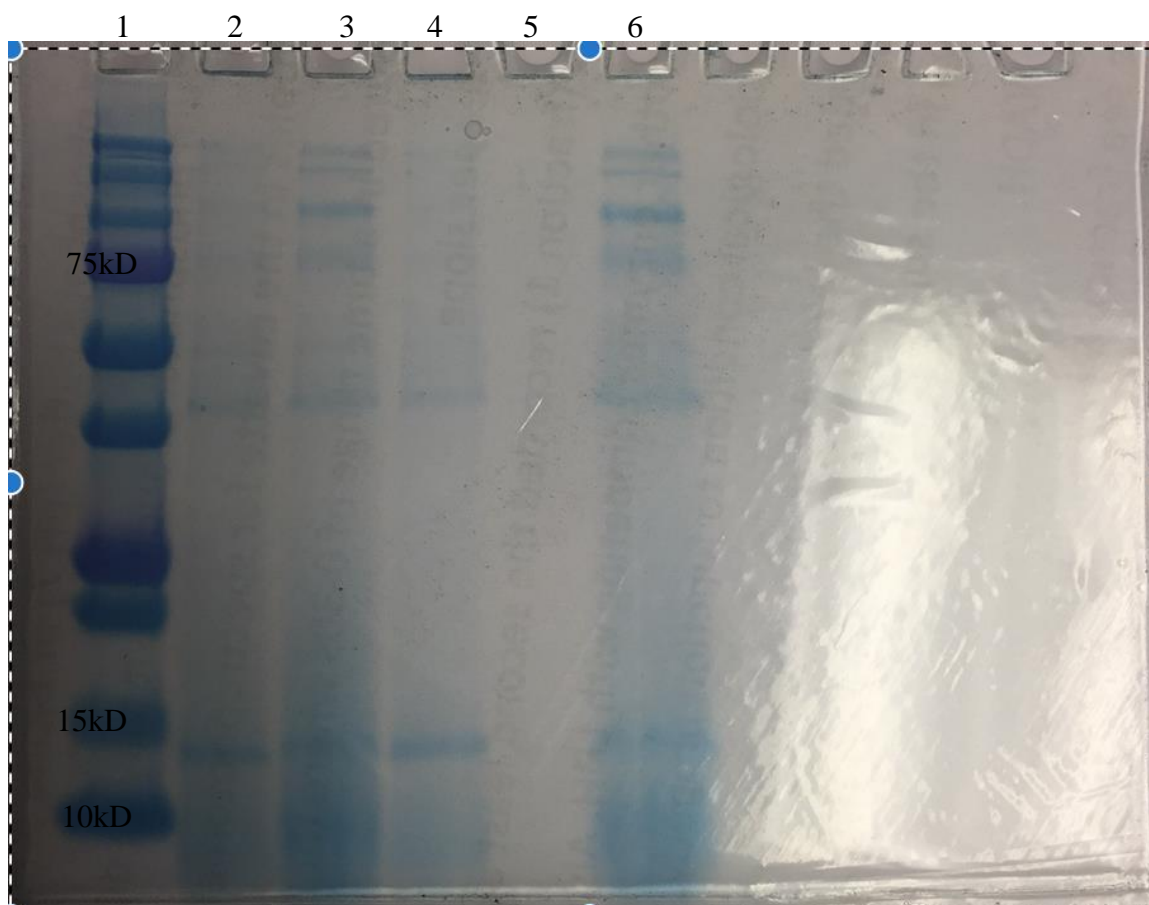


**Figure 3.3:** SDS-PAGE of the 96 h supernatant fractions from yeast grown at 28 °C. Protein was expressed at either 0.5% (v/v) or 1% (v/v) MeOH. Protein was precipitated with  $(\text{NH}_4)_2\text{SO}_4$ . The resulting precipitate was pelleted and dialyzed against 0.1 M KPi, pH 7. The samples were analyzed using a Mini-PROTEAN® TGX™ 8-16% ready-made gel from Bio-Rad. Lane 1: Precision Plus Standard Proteins from Bio-Rad. Lane 2: The dialyzed fraction originally grown at 0.5% (v/v) MeOH and precipitated with a 65%  $(\text{NH}_4)_2\text{SO}_4$  cut. Lane 3: The dialyzed fraction originally grown at 0.5% (v/v) MeOH and precipitated by raising the  $(\text{NH}_4)_2\text{SO}_4$  concentration from 65% to 85%. Lane 4: The dialyzed fraction originally grown at 1% (v/v) MeOH and precipitated with a 65%  $(\text{NH}_4)_2\text{SO}_4$  cut. Lane 5: empty. Lane 6: The dialyzed fraction originally grown at 1% (v/v) MeOH and precipitated by raising the  $(\text{NH}_4)_2\text{SO}_4$  concentration from 65% to 85%.

The remaining supernatant from the 65-85% cut was raised to 100% ammonium sulfate. The sample was then pelleted and dialyzed against 0.1 M KPi, pH 7. The resulting gel is shown in **Figure 3.4** below.

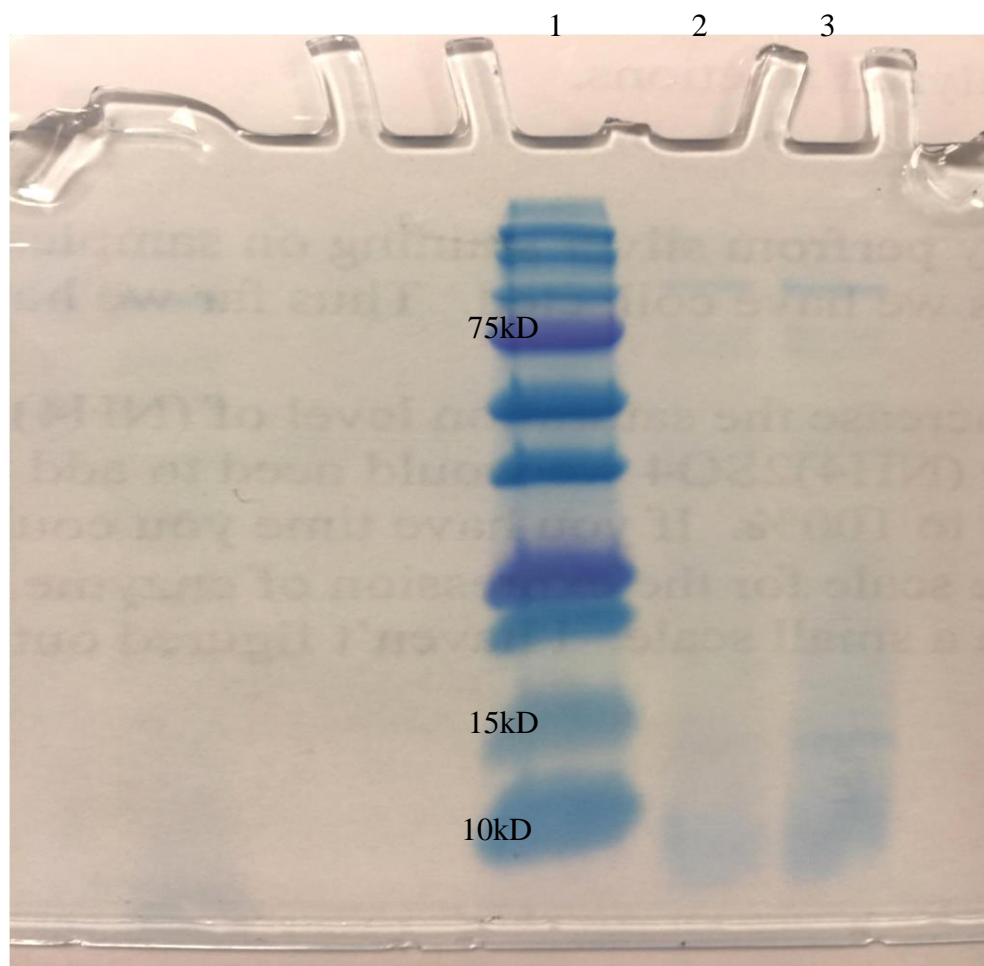


**Figure 3.4:** SDS-PAGE of the supernatant remaining after the 65-85% ammonium sulfate cut was raised to 100%  $(\text{NH}_4)_2\text{SO}_4$ . The resulting precipitate was pelleted and dialyzed against 0.1 M KPi, pH 7. The samples were analyzed using a Mini-PROTEAN<sup>®</sup> TGX<sup>™</sup> 8-16% ready-made gel from Bio-Rad. Lane 1: Precision Plus Standard Proteins from Bio-Rad. Lane 2: The dialyzed fraction originally grown at 0.5% (v/v) MeOH. Lane 3: The dialyzed fraction originally grown at 1% (v/v) MeOH.

Enzyme assays were conducted on the samples grown at different MeOH concentrations of 0.5% (v/v) or 1% (v/v) and raised to different  $(\text{NH}_4)_2\text{SO}_4$  concentrations.

The results are shown in **Table 3.5**.

**Table 3.5:** Determination of enzyme activity of 96 h fractions grown at either 0.5% (v/v) or 1% (v/v) MeOH and precipitated at different ammonium sulfate concentrations.

Sample (100 $\mu$ L)	[MeOH] (%)	(NH <sub>4</sub> ) <sub>2</sub> SO <sub>4</sub> Cut (%)	$\Delta$ A/min @ 450 nm	Units/mg
*Native HEWL			0.018	$2.40 \times 10^5$
T.3.4:1	0.5	65	-	<sup>†</sup> nd
T.3.4:2	0.5	85	0.025	$3.25 \times 10^3$
T.3.4:3	1	65	0.035	$7.60 \times 10^3$
T.3.4:4	1	85	0.038	$4.52 \times 10^3$

\*The native enzyme was diluted 100-fold for the enzyme assay.

<sup>†</sup>Enzyme activity was not detectable.

### ***Glycerol Concentration***

To determine the midpoint of the log phase, the *P. pastoris* X33-pPICZ $\alpha$ A-*hewl*H15S was grown with glycerol concentrations of either 0.5% (v/v) or 1% (v/v) in BMGY media. Growth in the BMGY media was performed at 28 °C. One mL samples were removed every hour and the OD<sub>600</sub> was measured. The results are given in **Table 3.6** showing the absorbance every 6 h. A plot of OD<sub>600</sub> vs time is given in **Figures 3.5A and B**.

**Table 3.6:** The growth of *P. pastoris* X33-pPICZ $\alpha$ A-hew/H15S in either 0.5% (v/v) or 1% (v/v) glycerol was monitored as OD<sub>600</sub> with time.

Time (Hs)	Absorbance @ OD <sub>600</sub> for 0.5% (v/v) GY	Absorbance @ OD <sub>600</sub> for 1.0% (v/v) GY
0	0	0
6	0.176	0.033
12	1.020	0.264
18	1.614	1.781
24	1.638	2.212
30	1.772	2.094

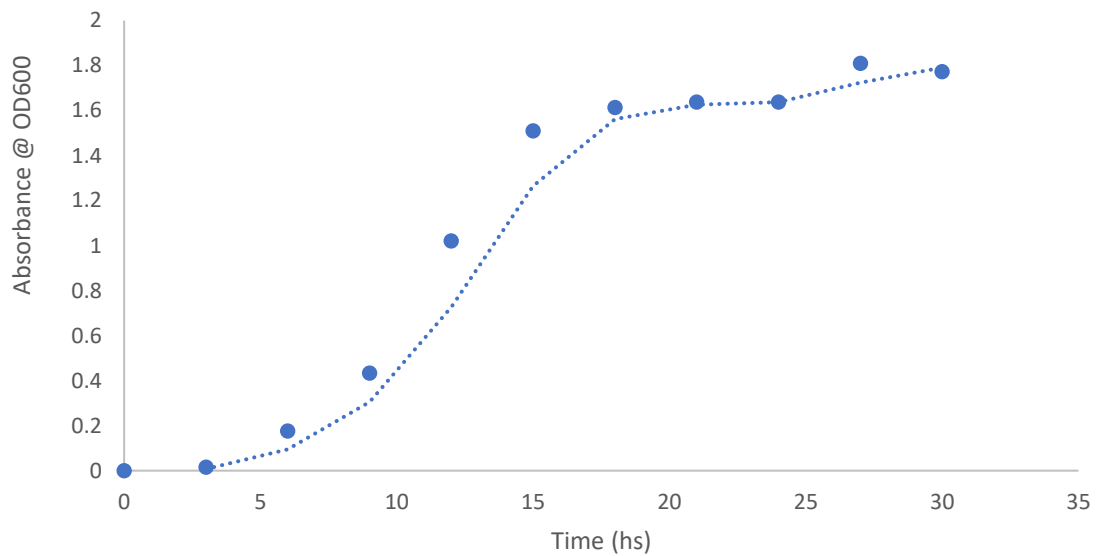


**Figure 3.5A:** Growth curve *P. pastoris* X33-pPICZ $\alpha$ A-hew/H15S grown in 0.5% (v/v) GY monitored as OD<sub>600</sub> with time (hs). Midpoint growth time was 13 h.



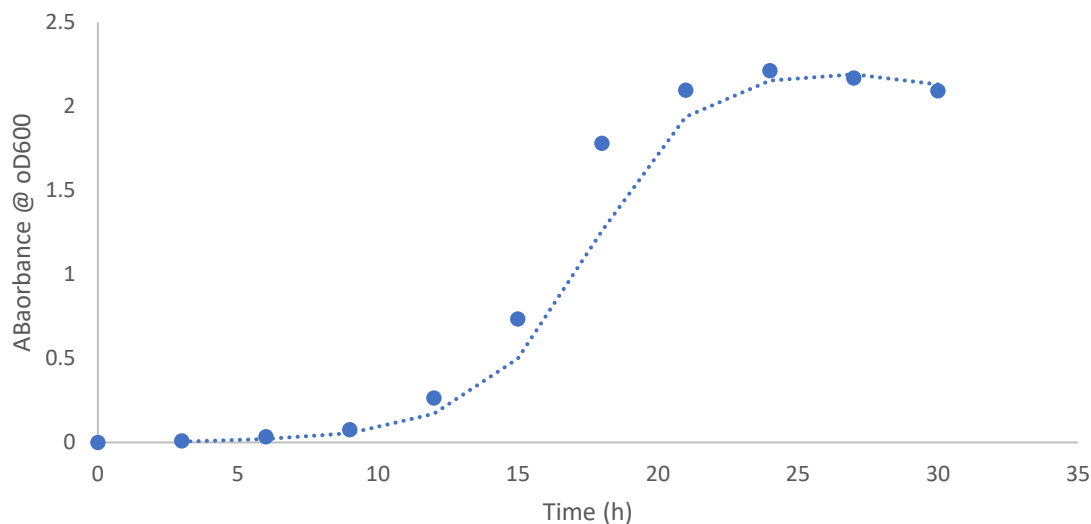


**Figure 3.5B:** Growth curve of *P. pastoris* X33-pPICZ $\alpha$ A-*hewlH15S* grown in 1% (v/v) GY monitored at OD<sub>600</sub> with time (hs). Midpoint growth time was 17 h.

#### *Protein Expression and Concentration*

After 13 h and 17 h growth of *P. pastoris* X33-pPICZ $\alpha$ A-*hewlH15S* in BMGY with two different concentrations of glycerol of 0.5% (v/v) and 1% (v/v) respectively, the cultures were transferred into BMMY media containing either 1% (v/v) or 2% (v/v) methanol. After 96 hs, the cells were harvested by centrifugation. Protein was precipitated from the supernatant in two stages. First the solutions were raised to 65% saturation with ammonium sulfate. After pelleting the precipitate by centrifugation, the remaining supernatant was raised to 85% saturation with ammonium sulfate. The precipitate in both cases was resuspended and dialyzed against 1 M KPi buffer, pH 7. A Bradford standard curve was generated using bovine serum albumin (BSA) as the protein standard. Protein expression of the samples was analyzed by SDS-PAGE. An enzyme assay was performed on each sample to measure activity. The results are shown in **Table 3.7** below.

**Table 3.7:** Bradford assay results for protein expressed with either 0.5% (v/v) or 1% (v/v) glycerol concentration and different concentration of MeOH - either 1% (v/v) or 2% (v/v).

Samples (50 $\mu$ L)	Time (h)	[GY] (%)	[MeOH] (%)	(NH <sub>4</sub> ) <sub>2</sub> SO <sub>4</sub> Cut (%)	Abs @595nm	[Protein] (mg/mL)
<b>Blank</b>					0	-
<b>BSA (10 <math>\mu</math>g)</b>					0.19	-
<b>BSA (30 <math>\mu</math>g)</b>					0.53	-
<b>BSA (50 <math>\mu</math>g)</b>					0.83	-
<b>BSA (70 <math>\mu</math>g)</b>					1.00	-
<b>T.3.7:1A</b>	24	0.5	1		0.18	0.19
<b>T.3.7:2A</b>	72	0.5	1		0.25	0.29
<b>T.3.7:3A</b>	96	0.5	1	85	0.18	0.18
<b>T.3.7:1B</b>	24	0.5	2		0.14	0.13
<b>T.3.7:2B</b>	72	0.5	2		0.33	0.40
<b>T.3.7:3B</b>	96	0.5	2	85	0.29	0.34
<b>T.3.7:1C</b>	24	1	1		0.07	0.04
<b>T.3.7:2C</b>	72	1	1		0.22	0.24
<b>T.3.7:3C</b>	96	1	1	85	1.04	1.37
<b>T.3.7:1D</b>	24	1	2		0.15	0.14
<b>T.3.7:2D</b>	72	1	2		0.22	0.24
<b>T.3.7:3D</b>	96	1	2	85	0.56	0.70

**Figures 3.6A-D** are the results of SDS-PAGE on the isolated and dialyzed fractions.

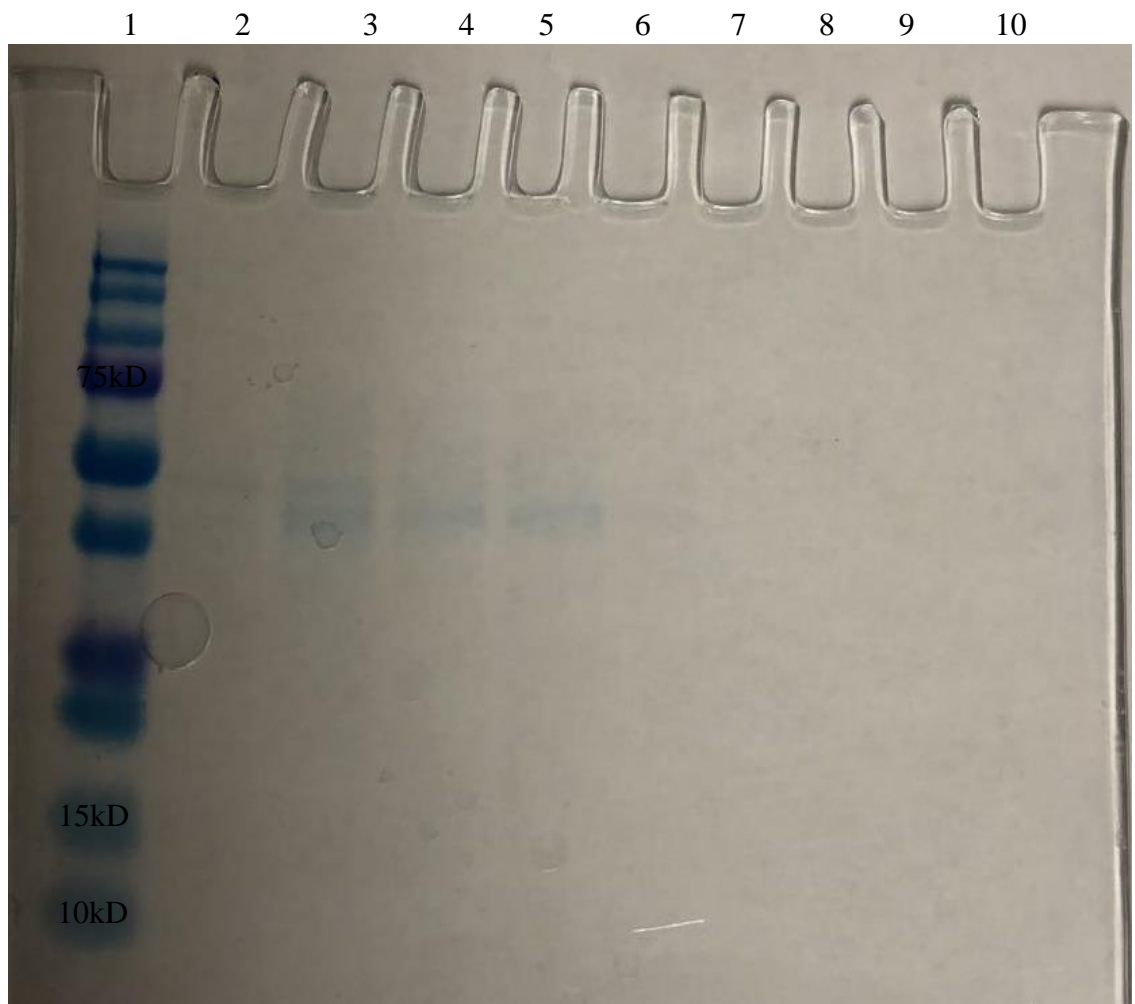


**Figure 3.6A:** SDS-PAGE analysis of aliquots collected from 25 to 96 h of the *P. pastoris* X33-pPICZ $\alpha$ A-*hew*/H15S strain initially expressed in 0.5% (v/v) GY BMGY media and transferred into 1% (v/v) MeOH BMMY media. Protein from approximately 95 mL of supernatant from the 96 h fraction was precipitated with  $(\text{NH}_4)_2\text{SO}_4$  and dialyzed against 0.1 M KPi, pH 7. All samples were analyzed using a Mini-PROTEAN® TGX™ 8-16% ready-made gel from Bio-Rad. Lane 1: Precision Plus Standard Proteins from Bio-Rad, Lane 2: 24 h sample aliquot, Lane 3: 48 h sample aliquot, Lane 4: 72 h sample aliquot, Lane 5: 96 h sample aliquot and Lane 6: 96 h sample aliquot precipitated with an 85% ammonium sulfate cut followed by dialysis against 0.1 M KPi, pH 7.

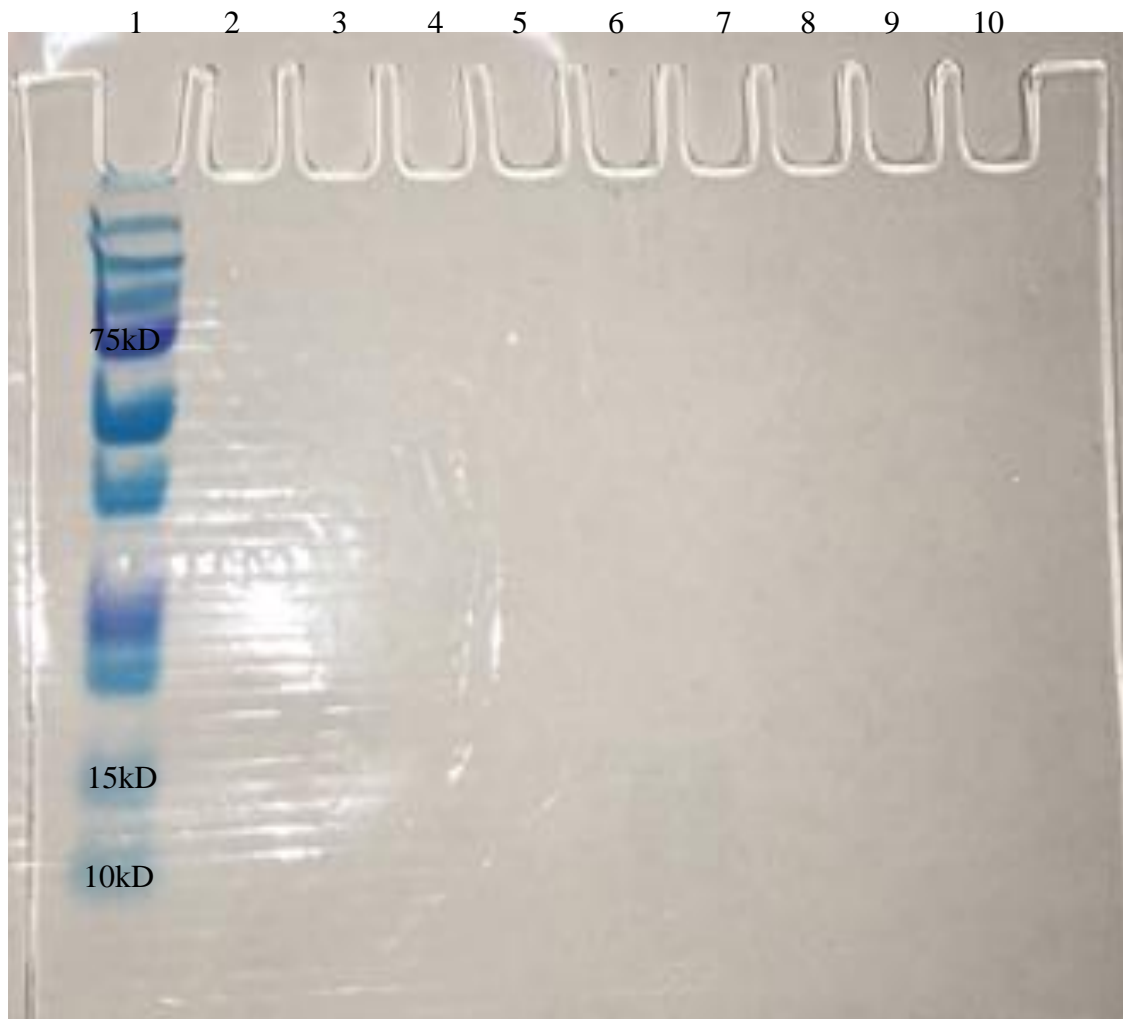


**Figure 3.6B:** SDS-PAGE analysis of aliquots collected from 24 to 96 h of the *P. pastoris* X33-pPICZ $\alpha$ A-*hew*/H15S strain initially expressed in 0.5% GY (v/v) BMGY media and transferred into BMMY at a 2% (v/v) MeOH concentration. Protein from approximately 95 mL of supernatant from the 96 fraction was precipitated with  $(\text{NH}_4)_2\text{SO}_4$  and was dialyzed against 0.1 M KPi, pH 7. All samples were analyzed using a Mini-PROTEAN<sup>®</sup> TGX<sup>™</sup> 8-16% ready-made gel from Bio-Rad. Lane1: Precision Plus Standard Proteins from Bio-Rad, Lane 2: 24 h sample aliquot, Lane 3: 48 h sample aliquot, Lane 4: 72 h sample aliquot, Lane 5: 96 h sample aliquot and Lane 6: 96 h sample aliquot precipitated with an 85% ammonium sulfate cut followed by dialysis against 0.1 M KPi, pH 7.

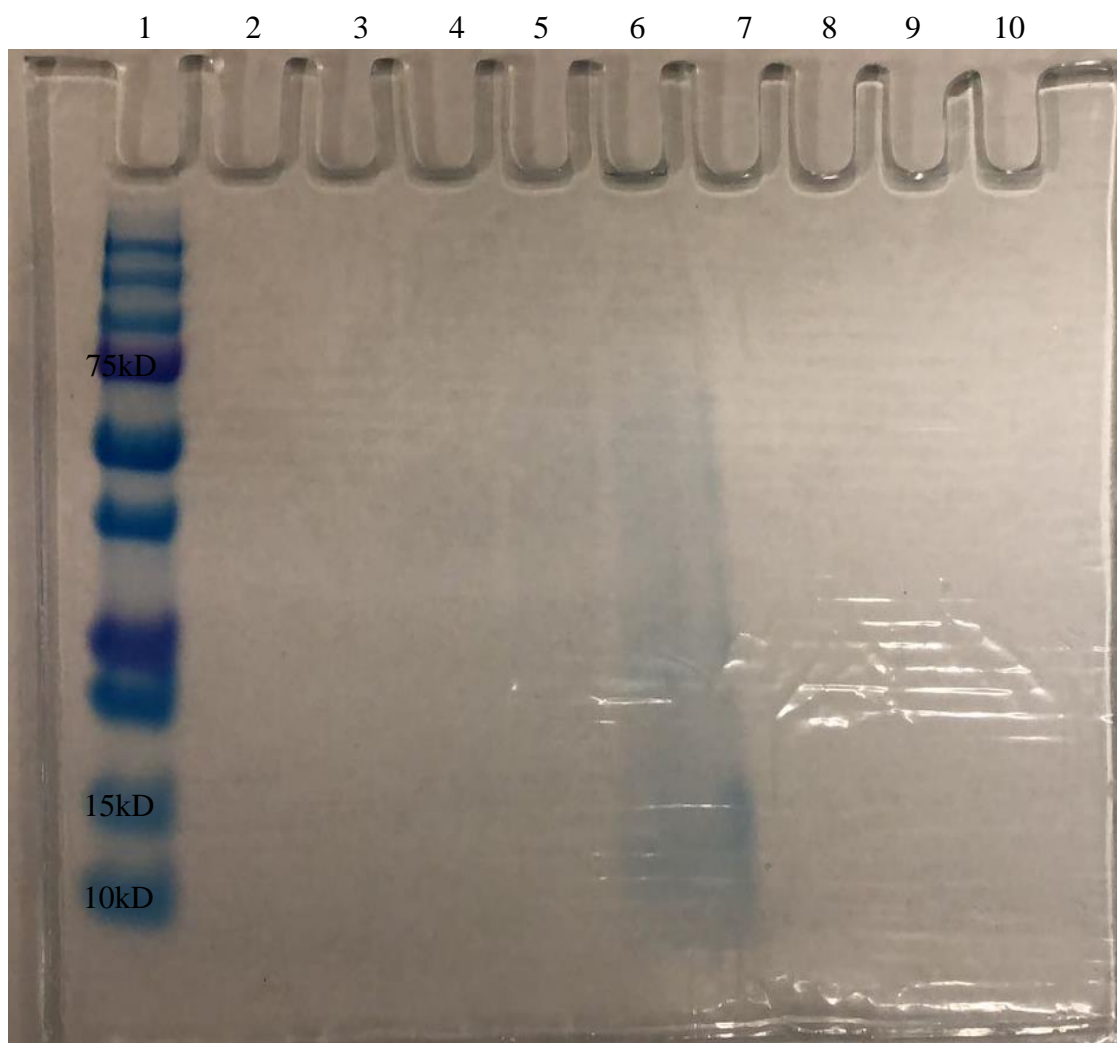


**Figure 3.6C:** SDS-PAGE analysis of aliquots collected from 24 to 96 h of the *P. pastoris* X33-pPICZαA-hew/H15S strain initially expressed in 1% GY (v/v) BMGY media and transferred into 1% (v/v) MeOH BMMY media. Protein from approximately 95 mL of supernatant from the 96 h fraction was precipitated with  $(\text{NH}_4)_2\text{SO}_4$  and dialyzed against 0.1 M KPi, pH 7. All samples were analyzed using a Mini-PROTEAN<sup>®</sup> TGX<sup>™</sup> 8-16% ready-made gel from Bio-Rad. Lane1: Precision Plus Standard Proteins from Bio-Rad, Lane 2: 24 h sample aliquot, Lane 3: 48 h sample aliquot, Lane 4: 72 h sample aliquot, Lane 5: 96 h sample aliquot and Lane 6: 96 h sample aliquot precipitated with an 85% ammonium sulfate cut followed by dialysis against 0.1 M KPi, pH 7.

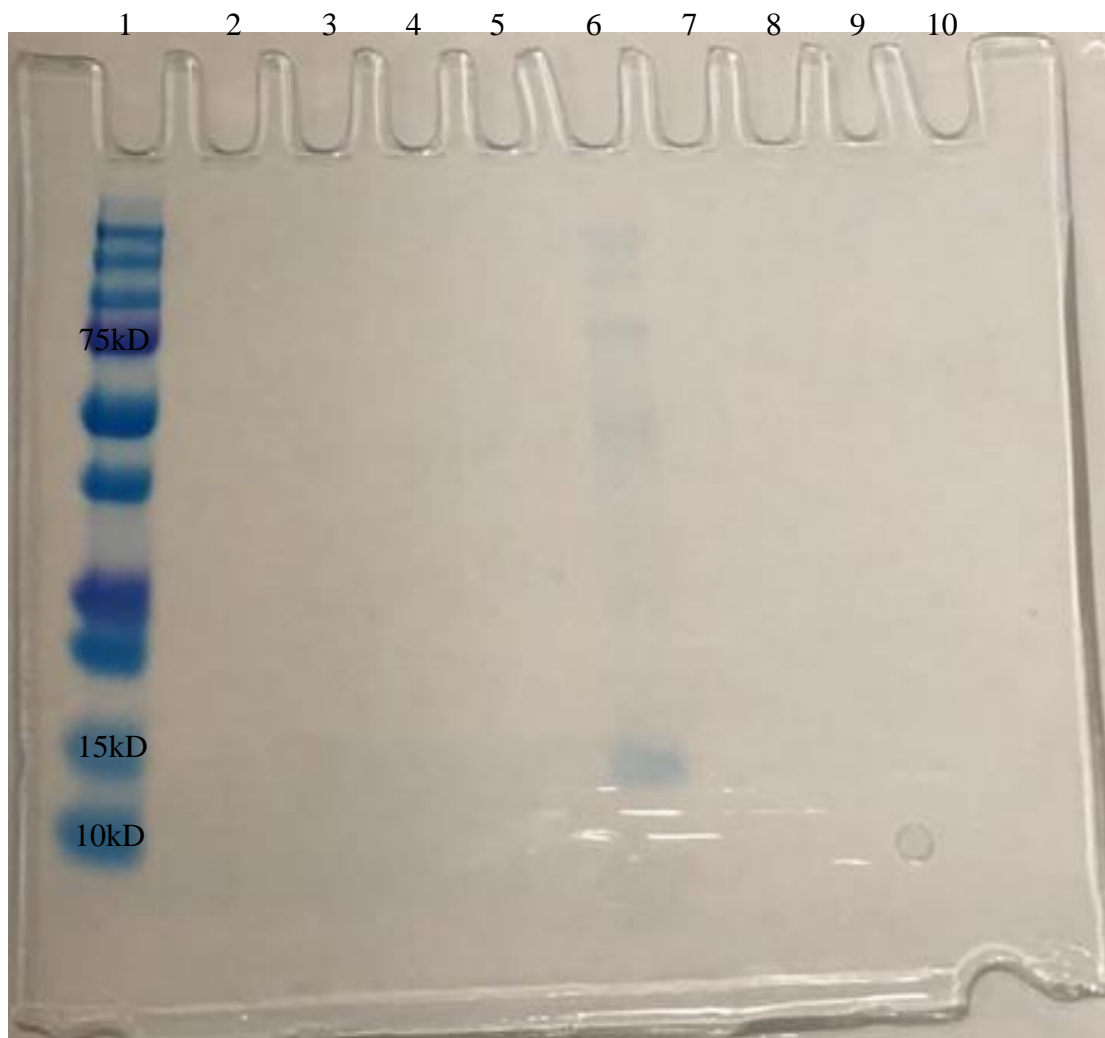


**Figure 3.6D:** SDS-PAGE analysis of aliquots collected from 24 to 96 h of the *P. pastoris* X33-pPICZ $\alpha$ A-*hewI*H15S strain initially expressed in 1% GY (v/v) BMGY media and transferred into 2% MeOH (v/v) BMMY. Protein from approximately 95 mL of supernatant from the 96 h fraction was precipitated with  $(\text{NH}_4)_2\text{SO}_4$  and dialyzed against 0.1 M KPi, pH 7. All samples were analyzed using a Mini-PROTEAN<sup>®</sup> TGX<sup>™</sup> 8-16% ready-made gel from Bio-Rad. Lane 1: Precision Plus Standard Proteins from Bio-Rad. Lane 2: 24 h sample aliquot, Lane 3: 48 h sample aliquot, Lane 4: 72 h sample aliquot, Lane 5: 96 h sample aliquot and Lane 6: 96 h sample aliquot precipitated with an 85% ammonium sulfate cut followed by dialysis against 0.1 M KPi, pH 7.

The turbidimetric enzyme assay results conducted on the samples are shown in

**Table 3.8** below.

**Table 3.8:** Turbidimetric enzyme assay of 96 h fractions for samples grown at different GY% and MeOH concentrations.

Sample (100 $\mu$ L)	$[(\text{NH}_4)_2\text{SO}_4]$ (%)	Time (h)	[GY] (%)	[MeOH] (%)	$\Delta A/\text{min}$ @450 nm	Units/mg
<b>Blank</b>					0.002	0
<b>*Native enzyme</b>					0.032	$4.15 \times 10^5$
<b>T.3.7:3A</b>	85	96	0.5	1	0.002	$1.33 \times 10^2$
<b>T.3.7:3B</b>	85	96	0.5	2	0.069	$2.02 \times 10^2$
<b>T.3.7:3C</b>	85	96	1	1	0.030	$2.17 \times 10^2$
<b>T.3.7:3D</b>	85	96	1	2	0.039	$5.58 \times 10^2$

\*The native enzyme was diluted 100-fold for the enzyme assay.

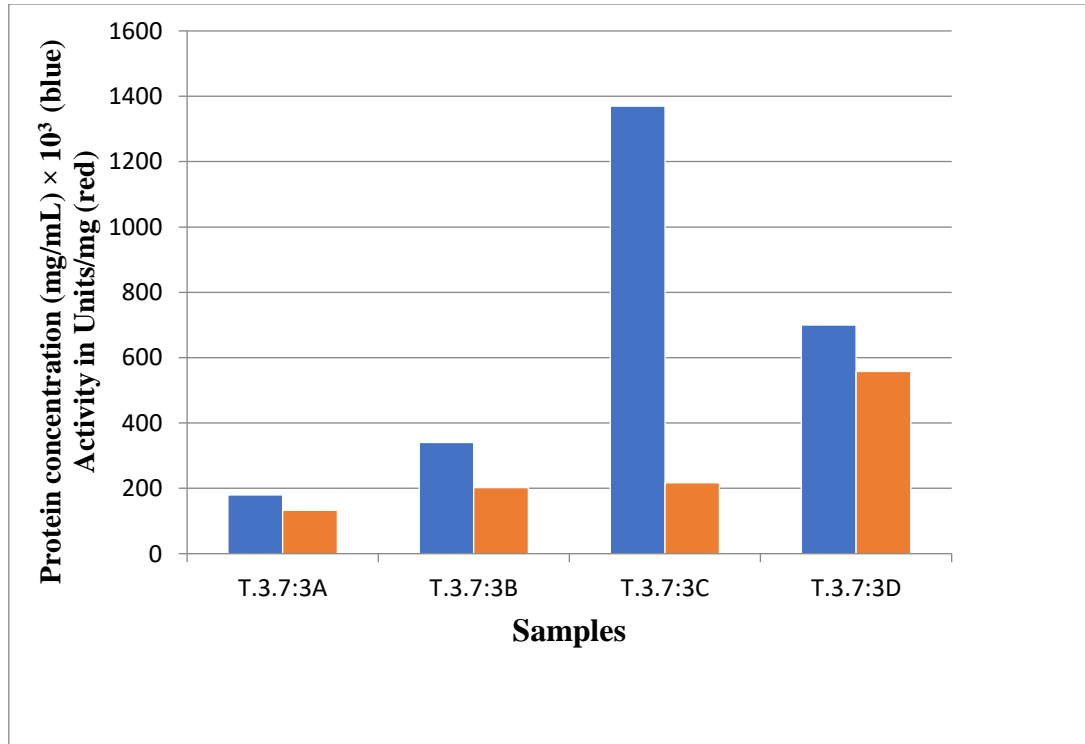


**Figure 3.7:** A histogram representation of protein concentration  $\times 10^3$  (mg/mL) (blue) and enzyme activity in Units/mg (orange).

### ***Intracellular Expression***

Intracellular protein expression was examined on 1 mL aliquots collected at 24 hour intervals over 96 hours to determine if any lysozyme activity remained in the cells. The cells were grown at 28 °C in a 0.5% (v/v) glycerol BMGY media and protein was expressed in either 0.5% (v/v) or 1% (v/v) MeOH BMMY media. The cells were lysed using Breaking buffer and acid washed glass beads and the resulting supernatant analyzed by SDS-PAGE (Figure 3.8).

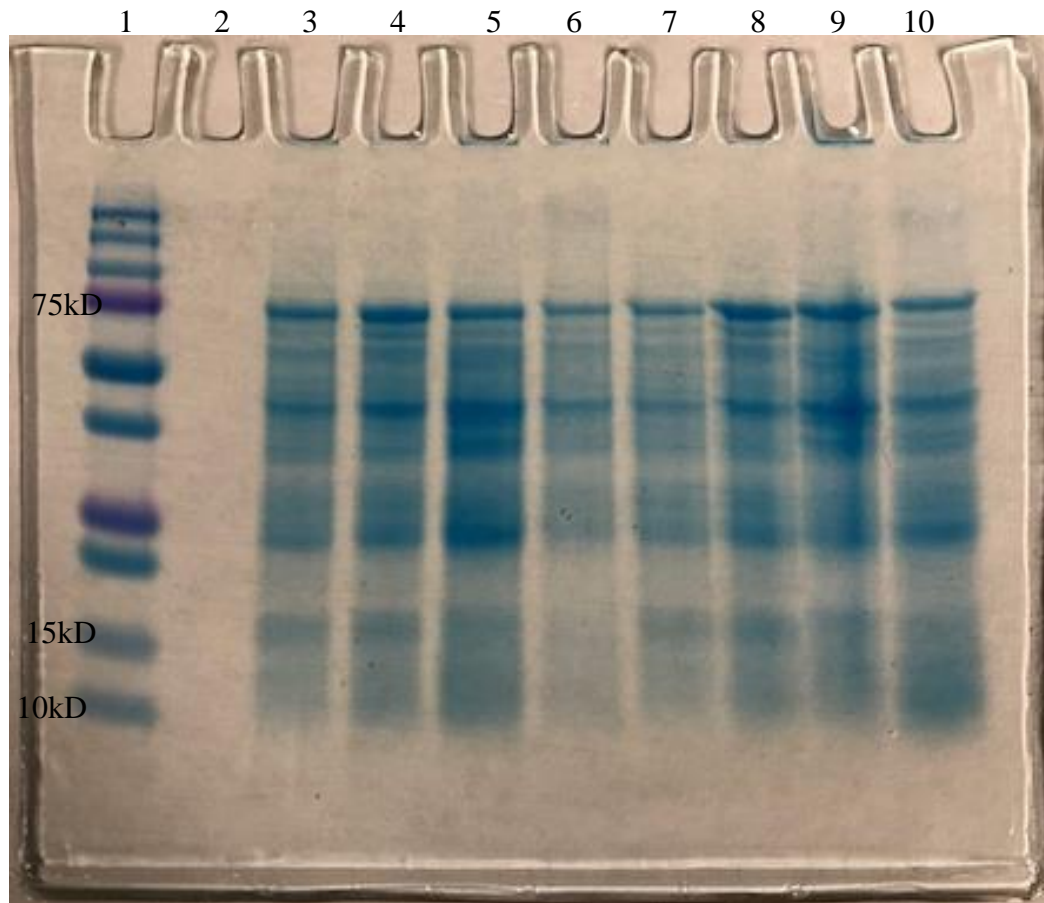


**Figure 3.8:** Supernatant of samples obtained from lysing cells grown at 0.5% (v/v) GY from 24 to 96 hours were analyzed using a Mini-PROTEAN® TGX™ 8-16% ready-made gel from Bio-Rad. Lane 1: Precision Plus Standard Proteins from Bio-Rad. Lane 2: empty. Lane 3-6: Protein expressed in buffered media, MES, pH 5.5 with EDTA and casamino acids after 24, 48, 72 and 96 hours respectively, grown at 0.5% MeOH. Lanes 7-10 same as Lanes 3-6 except protein was expressed in 1% MeOH.



### *Extracellular Expression vs Intracellular Expression at a Lower Temperature*

Different growth conditions were examined extracellularly and intracellularly for protein expression at a temperature of 22 °C. Conditions examined included addition of CaCl<sub>2</sub>, different MeOH concentrations, and the addition or elimination of EDTA in the BMMY media.

#### *Bradford Assay Extracellular Expression*

To examine both intracellular and extracellular expression, 1 mL fractions were collected at 24 h intervals. The cells were grown in 0.5% (v/v) GY BMGY media and protein were expressed in either 0.5% (v/v) or 1% (v/v) MeOH BMMY media with varying CaCl<sub>2</sub> and EDTA conditions. For intracellular expression, the collected fractions were thawed, and the cells were lysed using Breaking buffer and acid washed glass beads as described in Methods.

Intracellular protein expression was examined by SDS-PAGE. The resulting gels are shown in **Figures 3.9A and B**. All expression was performed at 22 °C.

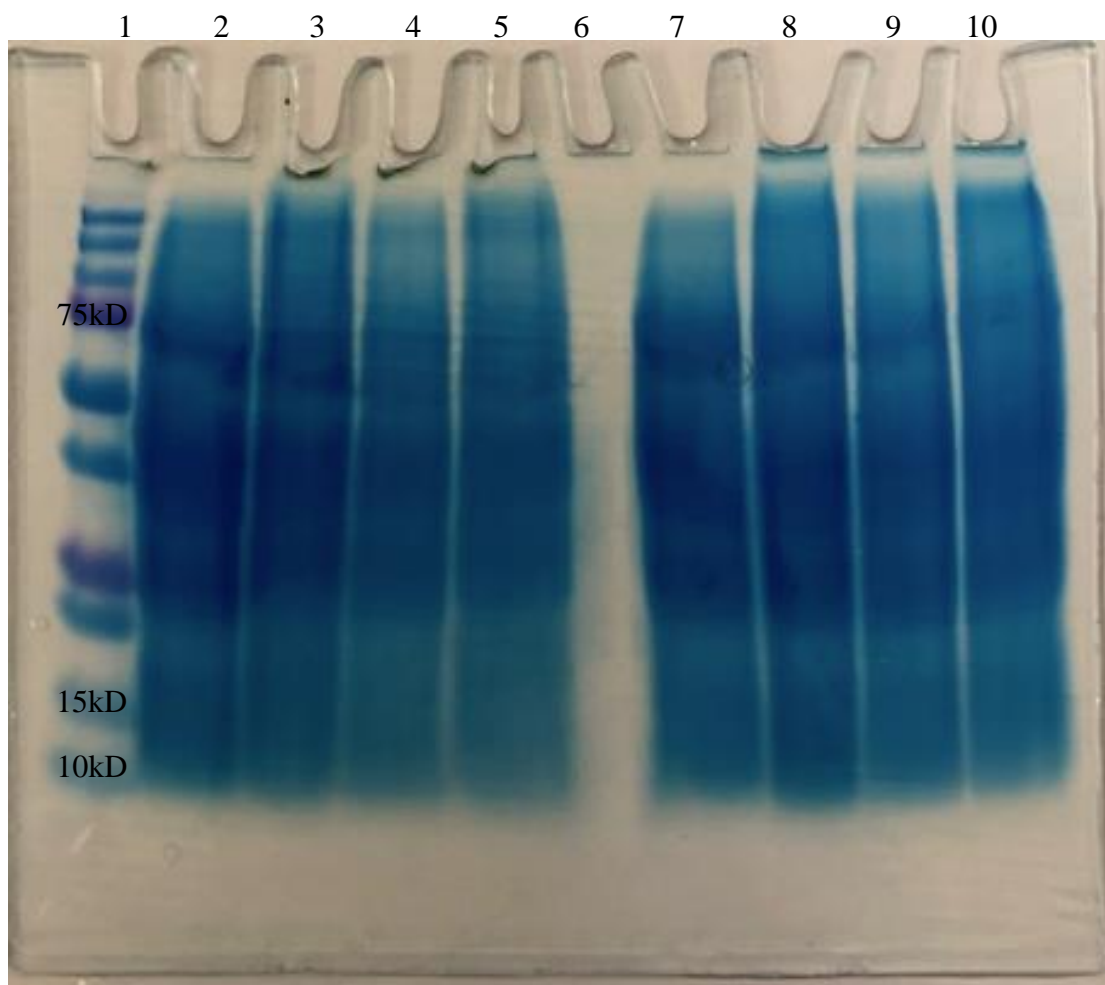


**Figure 3.9A:** SDS-PAGE of supernatant fractions of lysed cells at 24 h intervals from 24 to 96 h and initially grown at either 5% (v/v) or 1% (v/v) MeOH + CaCl<sub>2</sub> - EDTA. Fractions were analyzed using a Mini-PROTEAN<sup>®</sup> TGX<sup>™</sup> 8-16% ready-made gel from Bio-Rad. Lane1: Precision Plus Standard Proteins from Bio-Rad. Lanes 2, 3, 4 and 5: Protein expressed in buffered media , MES, pH 5.5 but without EDTA, at 24, 48, 72 and 96 hours respectively, grown at 0.5% MeOH. Lanes 6 is empty, Lanes 7, 8, 9 and 10: Protein expressed in buffered media containing same as above at 24, 48, 72 and 96 hours respectively, grown at 1% MeOH.

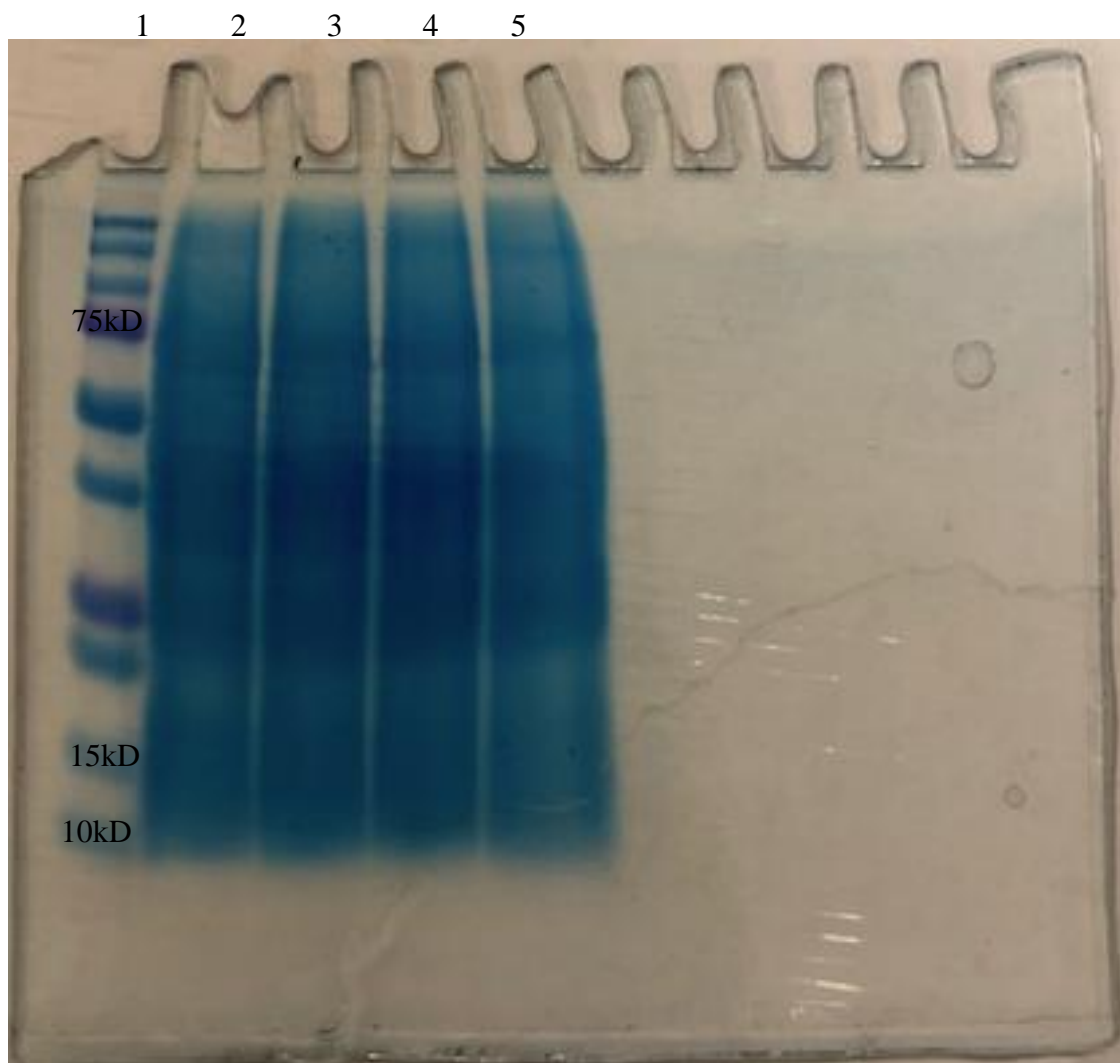


**Figure 3.9B:** SDS-PAGE of supernatant of lysed cells at 24 h intervals from 24 to 96 h and initially grown at 0.5% (v/v) MeOH + CaCl<sub>2</sub> + EDTA. Fractions were analyzed using a Mini-PROTEAN® TGX™ 8-16% ready-made gel from Bio-Rad. Lane1: Precision Plus Standard Proteins from Bio-Rad. Lanes 2, 3, 4 and 5: Protein expressed in buffered media, MES, pH 5.5 with EDTA, casamino acids and CaCl<sub>2</sub> after 24, 48, 72 and 96 hours respectively, grown at 0.5% (v/v) MeOH.

For extracellular expression, the supernatant of the collected 1 mL fractions at 24 h intervals from 24 to 96 h were analyzed. Also, the supernatant of the 96 h sample which was approximately 95 mL was raised to 85% ammonium sulfate saturation to precipitate protein. The precipitate was pelleted and then dialyzed against 0.1 M KPi, pH 7. The results are shown in **Table 3.9**.

**Table 3.9:** Determination of extracellular protein concentration expressed from yeast cells grown at 22 °C with varying growth conditions of EDTA, CaCl<sub>2</sub>, and MeOH concentration

SAMPLE (50 µl)	Time (h)	CaCl <sub>2</sub>	EDTA	[MeOH] (%)	Absorbance @ 595 nm	[Protein] (mg/mL)
<b>BSA (10 µg)</b>					0.265	-
<b>BSA (30 µg)</b>					0.573	-
<b>BSA (50 µg)</b>					0.913	-
<b>BSA (70 µg)</b>					1.225	-
<b>T.3.9:1A</b>	24	+	-	0.5	0.253	0.190
<b>T.3.9:2A</b>	48	+	-	0.5	0.425	0.404
<b>T.3.9:3A</b>	72	+	-	0.5	0.664	0.701
<b>T.3.9:4A</b>	96	+	-	0.5	0.864	0.949
<b>Precipitated T.3.9:4A</b>	96	+	-	0.5	1.024	1.147
<b>Precipitated T.3.9:4B</b>	96	+	-	1	0.848	0.929
<b>T.3.9:1C</b>	24	+	+	0.5	0.228	0.159
<b>T.3.9:2C</b>	48	+	+	0.5	0.335	0.292
<b>T.3.9:3C</b>	72	+	+	0.5	0.514	0.514
<b>T.3.9:4C</b>	96	+	+	0.5	0.820	0.895
<b>Precipitated T.3.9:4C</b>	96	+	+	0.5	0.978	1.091
<b>T.3.9:1D</b>	24	-	+	0.5	0.206	0.131
<b>T.3.9:2D</b>	48	-	+	0.5	0.339	0.297
<b>T.3.9:3D</b>	72	-	+	0.5	0.412	0.388
<b>T.3.9:4D</b>	96	-	+	0.5	0.401	0.374
<b>Precipitated T.3.9:4D</b>	96	-	+	0.5	1.146	1.299

The SDS-PAGE results of extracellular protein expression from samples collected at different time points and grown at different EDTA, CaCl<sub>2</sub> and MeOH concentrations are shown in **Figures 3.10A-C**. All expressions were performed at 22 °C.

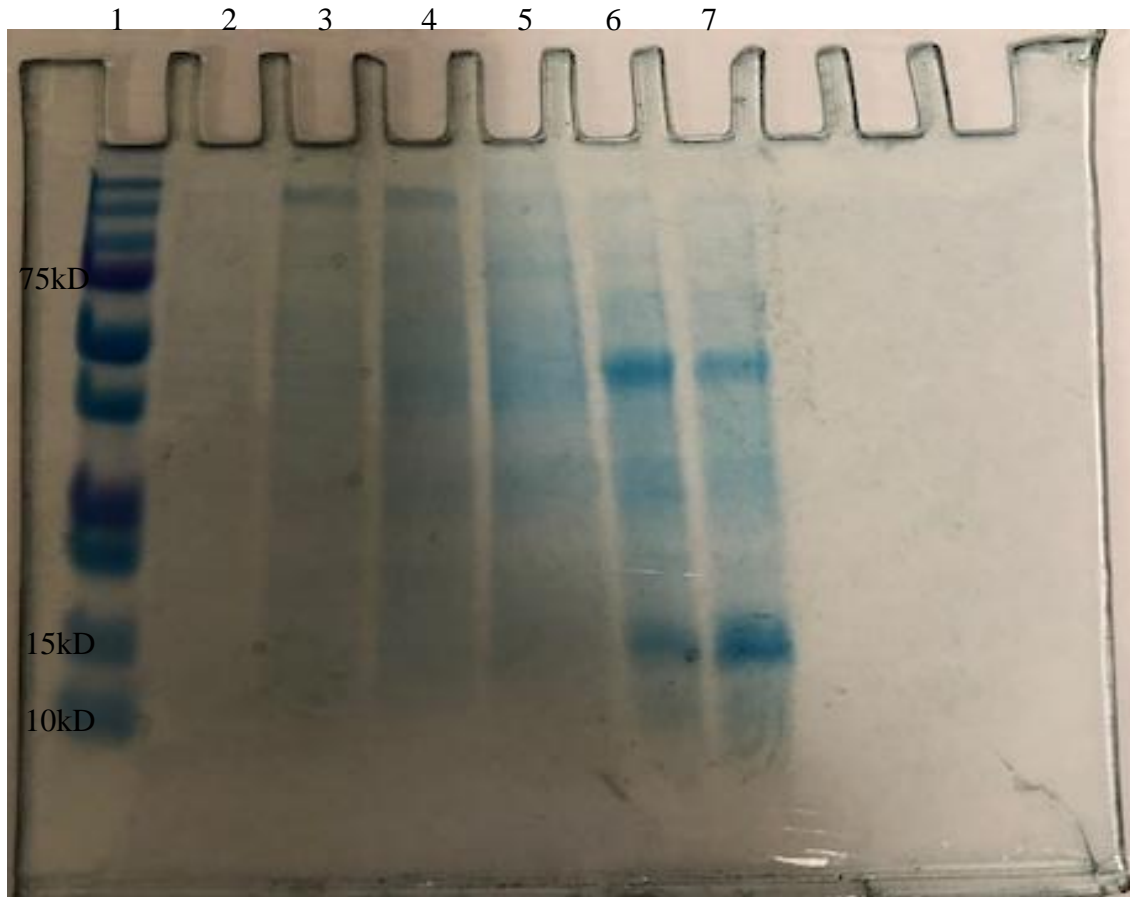


**Figure 3.10A:** SDS-PAGE of extracellular fractions at 24 time intervals from 24 to 96 h with protein expression in either 0.5% (v/v) or 1% (v/v) MeOH + CaCl<sub>2</sub> – EDTA. Fractions were analyzed using a Mini-PROTEAN<sup>®</sup> TGX<sup>™</sup> 8-16% ready-made gel from Bio-Rad. Lane1: Precision Plus Standard Proteins from Bio-Rad. Lanes 2, 3, 4 and 5: Protein expressed in buffered media, MES, pH 5.5 with casamino acids and CaCl<sub>2</sub> but without EDTA, after 24, 48, 72 and 96 hours respectively, grown at 0.5% (v/v) MeOH. Lanes 6 and 7: Dialyzed and concentrated 96 h supernatant grown at 0.5% (v/v) and 1% (v/v) MeOH respectively.

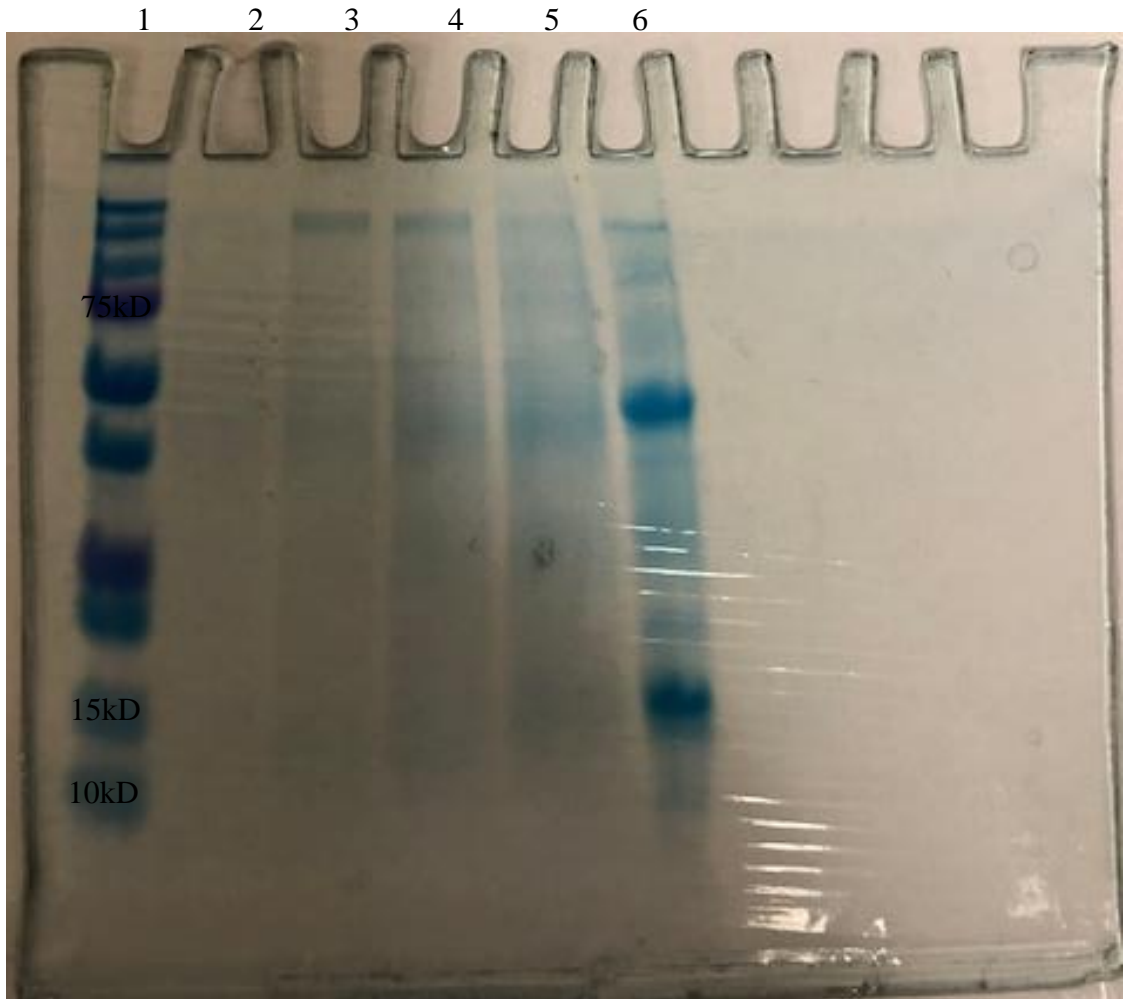


**Figure 3.10B:** SDS-PAGE of extracellular fractions at 24 time intervals from 24 to 96 h with protein expression at 0.5% (v/v) MeOH + CaCl<sub>2</sub> + EDTA. Fractions were analyzed using a Mini-PROTEAN<sup>®</sup> TGX<sup>™</sup> 8-16% ready-made gel from Bio-Rad. Lane 1: Precision Plus Standard Proteins from Bio-Rad. Lanes 2, 3, 4 and 5: Protein expressed in buffered media, MES, pH 5.5 with EDTA, casamino acids and CaCl<sub>2</sub> after 24, 48, 72 and 96 hours respectively, grown at 0.5% MeOH. Lane 6: Concentrated and dialyzed 96 h supernatant grown at 0.5% (v/v) MeOH.

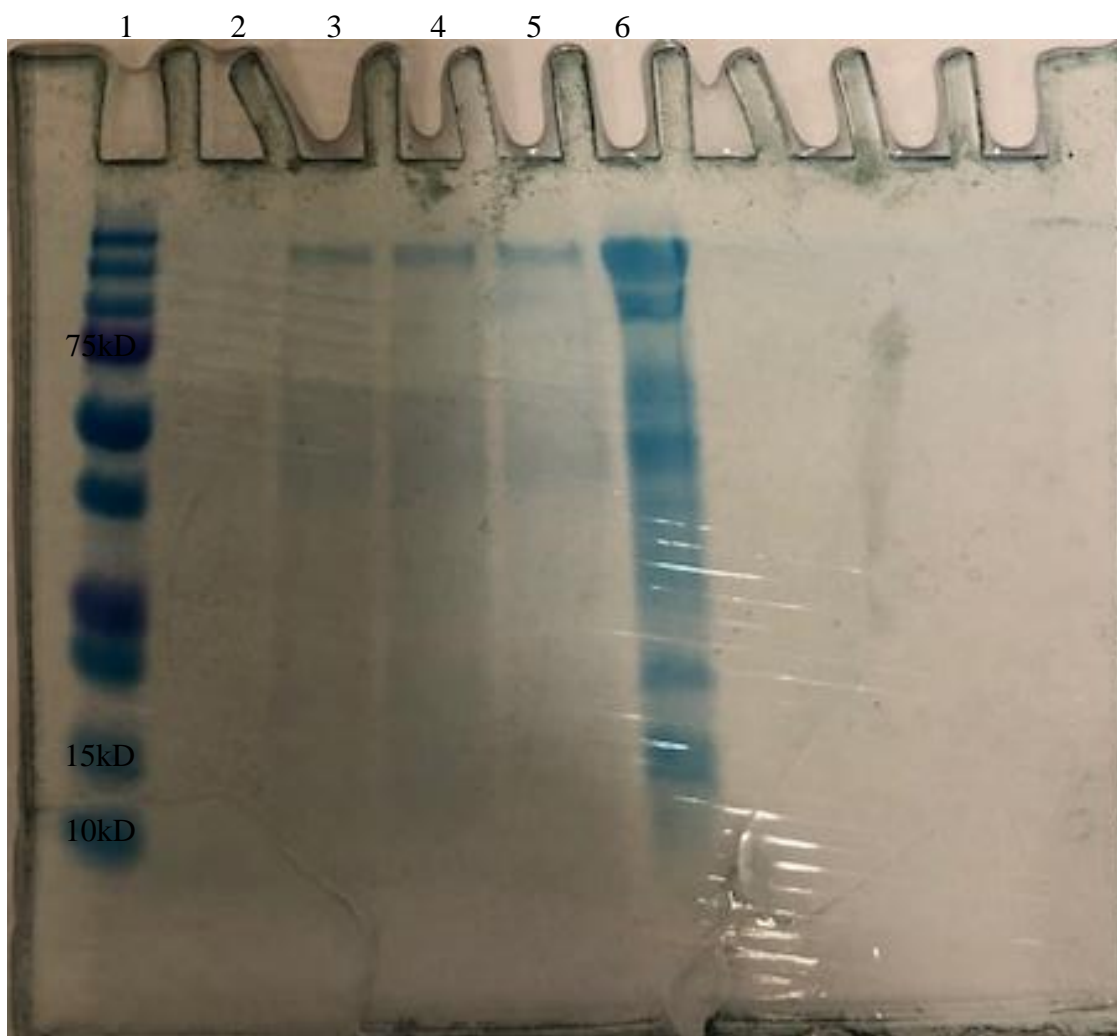


**Figure 3.10C:** SDS-PAGE of extracellular fractions at 24 time intervals from 24 to 96 h with protein expression 0.5% (v/v) MeOH - CaCl<sub>2</sub> + EDTA. Fractions were analyzed using a Mini-PROTEAN® TGX™ 8-16% ready-made gel from Bio-Rad. Lane 1: Precision Plus Standard Proteins from Bio-Rad. Lanes 2, 3, 4 and 5: Protein expressed in buffered media, MES, pH 5.5 with EDTA, casamino acids without CaCl<sub>2</sub> after 24, 48, 72 and 96 hours respectively, grown at 0.5% MeOH. Lanes 6: Concentrated and dialyzed 96 h supernatant grown at 0.5% (v/v) MeOH.

**Table 3.10** shows the results of enzyme assays performed on intracellular fractions under different growth conditions. All samples were grown at 22°C.

**Table 3.10:** Turbidimetric enzyme assays of intracellular fractions at 24 h intervals from 24 to 96 h from yeast grown at 0.5% (v/v) GY and different EDTA, CaCl<sub>2</sub> and MeOH concentrations.

Samples (100 $\mu$ L)	[MeOH] (%)	CaCl <sub>2</sub>	EDTA	Time (h)	$\Delta A/\text{min}$ @450 nm	Units
Blank					0	0
*Native enzyme (HEWL)					0.0434	$5.69 \times 10^7$
T.3.10:1A	0.5	+	-	24	-0.0027	<sup>‡</sup> nd
T.3.10:1B	0.5	+	-	48	0.0033	16.4
T.3.10:1C	0.5	+	-	72	0.0016	9.0
T.3.10:1D	0.5	+	-	96	-0.003	<sup>‡</sup> nd
T.3.10:2A	0.5	+	+	24	-0.0036	nd
T.3.10:2B	0.5	+	+	48	-0.004	nd
T.3.10:2C	0.5	+	+	72	-0.0029	nd
T.3.10:2D	0.5	+	+	96	-0.0029	nd
T.3.10:3A	0.5	-	+	24	-0.004	nd
T.3.10:3B	0.5	-	+	48	-0.0025	nd
T.3.10:3C	0.5	-	+	72	-0.0039	nd
T.3.10:3D	0.5	-	+	96	0.0001	0.47

\*The native enzyme was diluted 100-fold for the enzyme assay.

<sup>‡</sup>Enzyme activity was not detectable.

The results of the turbidimetric enzyme assays conducted to determine extracellular enzyme activity on the supernatant samples at different time points and different growth conditions of EDTA, CaCl<sub>2</sub> and MeOH concentrations are shown in **Table 3.11**.



**Table 3.11:** Turbidimetric enzyme assays of extracellular fractions at 24 h intervals from 24 to 96 h grown at 0.5% (v/v) GY and different EDTA, CaCl<sub>2</sub> and MeOH concentrations.

Sample	Time (h)	[MeOH] (%)	CaCl <sub>2</sub>	EDTA	ΔA/min @450	Units/mg
<b>Blank</b>					0	0
<b>*Native enzyme (HEWL)</b>					0.0434	5.69 × 10 <sup>5</sup>
<b>T.3.9:1A</b>	24	0.5	+	-	0.0038	2.00 × 10 <sup>2</sup>
<b>T.3.9:1B</b>	48	0.5	+	-	0.0098	2.42 × 10 <sup>2</sup>
<b>T.3.9:1C</b>	72	0.5	+	-	0.0232	3.30 × 10 <sup>2</sup>
<b>T.3.9:1D</b>	96	0.5	+	-	0.0144	1.52 × 10 <sup>2</sup>
<b>Precipitated T.3.9:1D</b>	96	0.5	+	-	0.1994	1.74 × 10 <sup>3</sup>
<b>Precipitated T.3.9:2D</b>	96	1	+	-	0.2623	2.82 × 10 <sup>3</sup>
<b>T.3.9:3A</b>	24	0.5	+	+	0.0082	5.17 × 10 <sup>2</sup>
<b>T.3.9:3B</b>	48	0.5	+	+	0.0178	6.07 × 10 <sup>2</sup>
<b>T.3.9:3C</b>	72	0.5	+	+	0.0297	5.78 × 10 <sup>2</sup>
<b>T.3.9:3D</b>	96	0.5	+	+	0.0436	4.88 × 10 <sup>2</sup>
<b>Precipitated T.3.9:3D</b>	96	0.5	+	+	0.2035	1.87 × 10 <sup>3</sup>
<b>T.3.9:4A</b>	24	0.5	-	+	0.0027	2.02 × 10 <sup>2</sup>
<b>T.3.9:4B</b>	48	0.5	-	+	0.0131	4.39 × 10 <sup>2</sup>
<b>T.3.9:4C</b>	72	0.5	-	+	0.0151	3.89 × 10 <sup>2</sup>
<b>T.3.9:4D</b>	96	0.5	-	+	0.0162	4.31 × 10 <sup>2</sup>
<b>Precipitated T.3.9:4D</b>	96	0.5	-	+	0.1575	1.21 × 10 <sup>3</sup>

\*The native enzyme was diluted 100-fold for the enzyme assay.

The *P. pastoris* X-33 yeast strain harboring the pPICZ $\alpha$ A vector was grown as a control. The growth conditions included initial growth at 0.5% GY (v/v) BMGY media followed by growth in either 0.5% (v/v) or 1% (v/v) MeOH BMMY media with shaking at 250 rpm and 22 °C. The protein was collected after 96 hs by precipitation using an 85% ammonium sulfate cut. The precipitate was dialyzed against 0.1 M KPi, pH 7 then examined by SDS-PAGE. The result is shown in **Figure 3.11**.

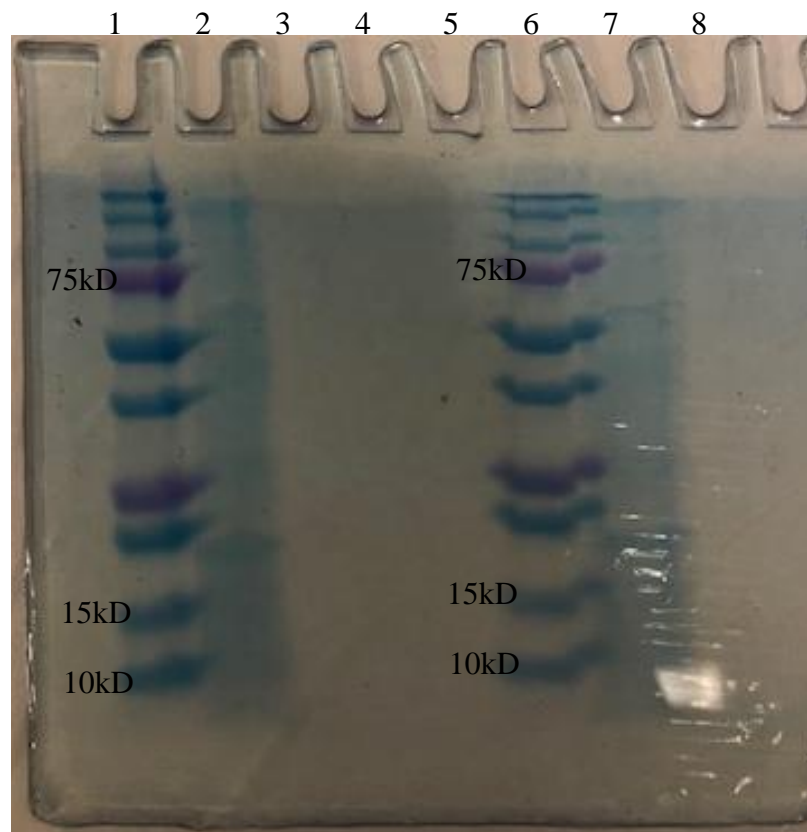


**Figure 3.11:** SDS-PAGE of extracellular proteins at 96 hs of growth precipitated at 85% (NH<sub>4</sub>)<sub>2</sub>SO<sub>4</sub> saturation. *P. pastoris* X-33 was transformed with pPICZ $\alpha$ A. The yeast was grown in 0.5% (v/v) GY BMMY media in either 0.5% (v/v) or 1% (v/v) MeOH. Lane 1 and Lane 6: Precision Plus Standard Proteins from Bio-Rad, Lane 2: 96 h fraction of *P. pastoris* X-33 transformed with pPICZ $\alpha$ A grown at 0.5% MeOH. Lane 7: 96 h fraction of *P. pastoris* X-33 transformed with pPICZ $\alpha$ A grown at 1% MeOH. Lanes 3, 4, 5 and 8: Empty.

The control did not show any lysozyme activity with the turbidimetric enzyme assay.

## CHAPTER 4: DISCUSSION

Previous work in Dr. Serra's lab generated a number of site-specific mutants of native hen egg white lysozyme. This research focused on optimizing the small scale expression of one of the mutants, H15S, using the *P. pastoris* expression system transformed with a recombinant pPICZ $\alpha$ A vector for extracellular expression of protein. The system has similar levels of protein processing, protein folding, and post-translational modification as eukaryotic expression systems and it is as easy to manipulate as *Saccharomyces cerevisiae* or *E. coli*. Other advantages in using this system compared to other eukaryotic expression systems such as baculovirus or mammalian tissue culture include lower cost, greater convenience and efficiency. According to K.M. Zsebo and colleagues, the *P. pastoris* expression system generated a 422-fold higher concentration of H5 lysozyme than that observed for *S. cerevisiae* which may be due to the high cell density growth of *P. pastoris*.<sup>56</sup> Also, R. Couderc and J. Baratti reported in their work that, *P. pastoris* grew to an OD<sub>600</sub> of 50, as compared to an OD<sub>600</sub> of 2.5 for *S. cerevisiae*. In addition, the extracellular expression of H5-lysozyme using *S. cerevisiae* and the signal peptide from lysozyme was only one-twentieth of that when the  $\alpha$ -factor signal sequence was used to secrete H15S-lysozyme in *P. pastoris*. Finally, *P. pastoris* expresses heterologous proteins at 10 to 100-fold higher levels than *S. cerevisiae* per the EasySelect™ *Pichia* Expression Kit, Version G, manual for expression of recombinant proteins using the pPICZ and pPICZ $\alpha$  plasmids for *Pichia pastoris*. Furthermore, the ability of the AOX1 promoter used in the *P. pastoris* expression to enable alcohol oxidase synthesis to levels higher than 30% of total soluble protein in methanol may be more efficient than the GPD promoter from *S. cerevisiae*.<sup>57</sup>

A single colony of the *P. pastoris* X33-pPICZαA-*hewl*H15S was grown on a YPD plate for 3 days and transferred into a 100 mL baffled flask containing 25 mL BMGY. The yeasts were first grown in a glycerol containing media, BMGY. The yeasts were transferred to a methanol containing media, BMMY, for protein expression. A variety of conditions were explored to increase growth of *P. pastoris* and protein expression. The effects of pH, percent glycerol, and temperature on the growth of yeast were examined. The percent methanol, temperature, and the presence or absence of CaCl<sub>2</sub> and EDTA were varied to gauge their effect on protein expression. Antifoam was added for better aeration. Different cuts of ammonium sulfate were used to determine the most effective amount to precipitate the mutant lysozyme.

The effect of pH on growth was explored. According to Brierley, Siegel, and coworkers, a pH of approximately 3 inhibits neutral proteases.<sup>58</sup> Use of BMGY media buffered at pH 5 resulted in poor growth of the yeast strain. The OD<sub>600</sub> was below 2 even after 24 hs as seen in **Table 3.1**. Media with a pH of 6 and above has also been explored in our lab, which resulted in increasing pH with time and the smell of decay in the culture. A pH of 5.5 has supported the growth of the yeast strain over 96 hs and was the pH used for the rest of the trials.

The effect of methanol and glycerol concentration on protein expression was examined. Cells were first grown in a BMGY media containing either 0.5% (v/v) or 1% GY. Yeast were then transferred to BMMY media with MeOH concentrations of 1% (v/v) or 2% (v/v) and sample fractions obtained from extracellular expression were analyzed. There was an increase in enzyme activity with an increase in methanol concentration as shown in **Figure 3.7**. Increasing methanol concentration from 1% (v/v) to 2% (v/v) resulted

in an increase in enzyme activity from  $1.33 \times 10^2$  Units/mg to  $2.02 \times 10^2$  Units/mg when the yeasts were initially grown in a 0.5% (v/v) GY media. When a 1% (v/v) GY media was used for initial growth the activity increased from  $2.17 \times 10^2$  Units/mg to  $5.58 \times 10^2$  Units/mg as the methanol concentration increased from 1% (v/v) to 2% (v/v). Initial growth with 1% (v/v) GY resulted in more total expressed protein while the use of 2% (v/v) MeOH correlated with the highest enzyme activity in units per mg. This suggests that most of the expressed protein under these conditions was likely the H15S lysozyme mutant. SDS-PAGE showed a band in between the 10 kD and 15 kD molecular mark in both the 1% (v/v) and 2% (v/v) MeOH concentrations. (**Figures 3.6C and 3.6D**).

Low protein concentrations and weak bands on SDS-PAGE lead us to the use of ammonium sulfate to precipitate protein from the approximately 90 – 95 mL of supernatant remaining after 96 h of growth. Significant enzyme activity was observed at both the 65% and 65% to 85% ammonium sulfate cuts. Also, SDS-PAGE showed distinct bands corresponding to about 14.4 kD when the enzyme was expressed in either 0.5% (v/v) or 1% (v/v) MeOH with both ammonium sulfate cuts. Only a faint band at about 14 kD appeared when the 1% (v/v) MeOH supernatant was raised from 85% to 100% (**Figure 3.3 and 3.4**). We decided to precipitate the protein from the 96 h supernatant using 85% ammonium sulfate for the rest of our work.

To further examine low protein expression, we explored the use of different GY concentrations in BMGY on the growth of the yeast. A plot of OD<sub>600</sub> vs time at two different GY concentrations is given in **Figures 3.5A and 3.5B**. BMGY media with 0.5% (v/v) GY showed a faster rate of growth as compared to the 1% (v/v) GY media though the 1% (v/v) media did result in a higher OD<sub>600</sub> with time. In both cases, the mid-point of the

log phase occurred at an OD<sub>600</sub> of about 1. This is only half of the expected OD<sub>600</sub> for mid-log growth. We grew the yeast to an OD<sub>600</sub> of about 2.0 for our initial experiments as recommended by the manufacturer. By that time the yeasts were in the stationary phase of growth. This likely explains why the expression of protein was relatively poor for the first set of experiments. The 0.5% (v/v) and 1% (v/v) GY growth curves reached their mid-point at different times - 13 h and 17 h, respectively. Cells were grown to an OD<sub>600</sub> of 1 in BMGY media instead of 2 for the remaining experiments.

We next investigated intracellular expression to see if the mutant lysozyme was being retained within the cell. Frozen cells from previous growth in 0.5% GY (v/v) BMGY and either 0.5% (v/v) or 1% (v/v) MeOH BMMY media were thawed and lysed open using acid washed beads and Breaking Buffer. The mixture was centrifuged, and SDS-PAGE performed on the supernatant. (**Figure 3.8**).

A diffuse band appears around 15 kD. Lane 4 appears to show two faint bands with one at about 15 kD and one slightly higher. Akira Saito et al. observed in their lysozyme secreted from *P. pastoris* the native enzyme plus a version that was 9 residues longer.<sup>67</sup> They proposed the longer protein was due to differential cleavage of the signal peptide by the yeast protease Kex2. The Kex2 protease cleaves to the carboxyl side of either Arg-Arg or Lys-Arg and functions at pHs as low as pH 5 but has an optimum pH of 9 and an optimum temperature of 37 °C. Also, Kex2 is Ca<sup>2+</sup> dependent. This is important because we have been using EDTA in our media to inhibit protease activity. EDTA chelates Ca<sup>2+</sup> which might have an effect on the activity of Kex2 protease.<sup>59-64</sup> We explored the effect of CaCl<sub>2</sub> and EDTA on protein expression.

It may be difficult to separate effects of temperature and CaCl<sub>2</sub> on protein expression. CaCl<sub>2</sub> in either the presence or absence of EDTA generated nearly 1 mg/mL of extracellular protein at 96 h (**Table 3.9**). By comparison the protein concentration of extracellular protein of the 96 h sample without CaCl<sub>2</sub> was less than half that at 0.37 mg/mL. The enzyme activity for the three conditions in the precipitated 96 h samples from **Table 11** showed the presence of CaCl<sub>2</sub> and EDTA measuring the highest enzyme activity of  $1.87 \times 10^2$  Units/mg compared to the other conditions which measured  $1.74 \times 10^2$  Units/mg (CaCl<sub>2</sub> present but no EDTA) and  $1.21 \times 10^2$  (EDTA present but no CaCl<sub>2</sub>). In general, high enzyme activity is seen in the 24-96 h aliquot samples with both CaCl<sub>2</sub> and EDTA present followed by samples with EDTA present but no CaCl<sub>2</sub>. However, highest enzyme activity from **Table 11** is seen in the precipitated 96 h sample with CaCl<sub>2</sub> present but no EDTA at 1% (v/v) MeOH ( $2.82 \times 10^2$  Units/mg).

The closest comparison that can be made regarding temperature involves the conditions listed in **Table 3.7**. Cells were grown at 28 °C and protein was expressed in a 1% (v/v) MeOH BMMY media. This is close to the conditions in which the cells were grown at 22 °C with EDTA, without CaCl<sub>2</sub> in a 0.5% (v/v) MeOH media. Precipitation of extracellular protein with an 85% saturated ammonium sulfate solution at 96 h gave 0.18 mg/mL of protein when the cells were grown at 28 °C and 1.30 mg/mL of protein when grown at 22 °C. Lowering the temperature appears to have greatly reduced the amount of intracellular lysozyme as can be seen by comparing Figures 3.8 and 3.9. Lysozyme activity was essentially undetectable under all growth conditions (**Table 3.10**). Lower temperature may allow for more efficient folding and secretion of the enzyme.

## CONCLUSION

“Caged type” reactions occur when transition metal ions in a protective pocket formed from the tertiary structure of proteins bind the surface of the protein to produce ROS. The pocket provides protection for the ROS generated from anti-oxidants and leads to oxidative damage by ROS. It is known that some amino acid residues such as histidine and methionine have high affinity for transition metals and are more susceptible to oxidation. Perhaps, all that is needed for site-specific oxidative damage is the presence of these amino acids in the primary structure and tertiary structure is not important. A few HEWL mutants have been developed in the lab to examine the effect of structure on site-specific oxidation. To date, the amount of extracellular protein expressed has been too little for studying MCO systems. This thesis examined the optimization of the small scale expression of H15S, one of the mutants of HEWL developed using the *Pichia pastoris* expression kit system.

The *P. pastoris* X33-pPICZ $\alpha$ A-*hewl*H15S strain was subjected to a variety of growth conditions and a number of variables were explored to increase extracellular protein expression. Both intracellular and extracellular protein expression were examined and analyzed for enzyme activity. High glycerol concentration of 1% (v/v) showed a higher protein concentration as compared to 0.5% (v/v) as shown in **Figure 3.7**. Increasing the methanol concentration resulted in an increase in enzyme activity in Units per mg. However, an increase in methanol concentration was not consistent with an increase in protein concentration. Precipitation of protein by ammonium sulfate showed a 85% ammonium sulfate concentration to be optimal for protein isolation. In addition, conditions with CaCl<sub>2</sub> present also showed more protein concentration and enzyme activity than



conditions without. Finally, growing the culture in the buffered media at a lower temperature of 22 °C increased both protein concentration and enzyme activity for all conditions. This may support Dagang Huang and colleagues work that the coupled process of protein folding and synthesis with secretory trafficking is better achieved at lower temperature of 20 °C.

Future work will be focused on the optimal temperature for expression and HPLC confirmation of the mutant HEWL, H15S. Also, the H15S mutant will be subjected to a metal-catalyzed oxidation system and analysis and compared to the oxidation of the native enzyme, HEWL.

## REFERENCES

1. <http://www.vivo.colostate.edu/hbooks/pathphys/topics/radicals.html>
2. Bandyopadhyay, U., Das, and Banerjee, R.K., *Curr. Sci. India.*, 1999, **77**, 658-666.
3. Harman, D., *Drug Aging*, 1993, **3**, 60-80.
4. Fridovich, I., *Annu. Rev. Pharmacol. Toxicol.*, 1983, **23**, 29-257.
5. Turrens, J.F and Boveris, A., *Biochem. J.*, 1980, **191**, 421-427.
6. Fenton, H.J.H., *J. Chem. Soc. Trans.* 1984, **65**, 899-911.
7. Reuter, S., Gupta, S.C., Chaturvedi, M.M., Aggarwal, B.B., *Free Rad. Bio. Med.* 2010, **49**, 1603-1616.
8. Thomas, C. E. and Kalyanaraman, B. (eds), in *Oxygen Radicals and the Disease Process*, Hardwood Academic Publishers, The Netherlands, 1997.
9. Fridovich, I., *Annu. Rev. Pharmacol. Toxicol.*, 1983, **23**, 29-257.
10. Fridovich, I., *Arch. Biochem. Biophys.*, 1986, **247**, 1-11.
11. Blake, D. R., Allen, R. E. and Lunec, J., *Br. Med. Bull.*, 1987, **43**, 371-385.
12. Weitzman, S. A., Turk, P. W., Milkowski, D. H. and Kozlowski, K., *Proc. Natl. Acad. Sci. USA*, 1994, **91**, 1261-1264.
13. Counts, J. L. and Goodman, J. I., *Mol. Carcinogenesis*, 1994, **11**, 185-188.
14. Halliwell, B. and Gutteridge, J. M. C., *Methods Enzymol.*, 1990, **186**, 1-85.
15. Chevion, M., Jaing, Y., Har-El, R., Berenshtein, E., Uretzky, G. and Kitrossky, N., *Proc. Natl. Acad. Sci. USA*, 1993, **90**, 1102-1106.
16. Hedlund, B. E. and Hallway, P. E., *Biochem. Soc. Trans.*, 1993, **21**, 340-343.
17. Das, D., Bandyopadhyay, D., Bhattacharjee, M. and Banerjee, R. K., *Free Rad. Biol. Med.*, 1997, **23**, 8-18.
18. Schapira, A. V. H., Hartley, A., Cleeter, M. W. J. and Cooper, J. M., *Biochem. Soc. Trans.*, 1993, **21**, 367-370.

19. Fairburn, K., Stevens, C. R., Winyard, P. G., Kus, M., Ward, R. J., Cunningham, J., Zaidi, M. and Blake, D. R., *Biochem. Soc. Trans.*, 1993, **21**, 371–375.
20. McCord, J. M., *Fed. Proc. Fed. Am. Soc. Exp. Biol.*, 1987, **46**, 2402.
21. Halliwell, B. and Gutteridge, J. M. C., *Biochem. J.*, 1984, **219**, 1–14.
22. Earl R. Stadtman and Barbara S. Berlett, *Chem. Res. Toxicol.*, 1997, **10**, 485-494.
23. Stadtman, E.R., *Free Rad.Bio. Med.*, 1990, **9**, 315-325.
24. Skulachev, V. P., *Quart. Rev. Biophys.*, 1996, **29**, 169-202.
25. Clémence Cheignon Peter Faller Denis Testemale, Christelle Hureau, and Fabrice Collin, *Metallomics*, 2016, **8(10)**, 1081-1089.
26. Dean, R. T., Fu, S., Stocker, R., and Davies, M. J., *Biochem. J.*, 1997, **324**, 1-18.
27. Stadtman, E. R., *Free Radicals, Oxidative Stress, and Antioxidants* (Ozben, ed.) Academic Plenum Press, N.Y., 1998, pp. 51-64.
28. Stadtman, E. R., and Levine, R. L., *Amino Acids*, 2003, **25**, 207-218.
29. Barbara S. Berlett and Earl R. Stadtman, *The Journal of Biological Chemistry*. 1997, **272**, 20313-20316.
30. Garrison, W. M., *Chem. Rev.* 1987, **87**, 381–398.
31. Schuessler, H., and Schilling, K., *Int. J. Radiat. Biol.*, 1984, **45**, 267–281.
32. Uchida, K., Kato, Y., and Kawakishi, S., *Biochem. Biophys. Res. Commun.*, 1990, **169**, 265–271.
33. Schuenstein, E., and Esterbauer, H., *CIBA Found. Symp.*, 1979, **67**, 225–244
34. Esterbauer, H., Schaur, R. J., and Zolner, H., *Free Radical Biol. Med.*, 1991, **11**, 81–128.
35. Uchida, K., and Stadtman, E. R., *J. Biol. Chem.*, 1993, **268**, 6388 – 6393.
36. Kristal, B. S., and Yu, B. P., *J. Gerontol.*, 1992, **47**, 104 –107
37. Baynes, J. W. *Diabetes*, 1996, **40**, 405– 411
38. Monnier, V., Gerhardinger, C., Marion, M. S., and Taneda, S., *Oxidative Stress and Aging*, 1995 (Cutler, R. G., Packer, L., Bertram, J., and Mori, A., eds) 141–149, Birkhauser Verlag, Basel, Switzerland.

39. Levine, R. L., Williams, J. A., Stadtman, E. R., and Schacter, E., *Methods Enzymol.*, 1994, **233**, 346–357.
40. Barbara S. Berlett and Earl R. Stadtman, *The Journal of Biological Chemistry.*, 1997, **272**, 20313-20316.
41. Pryor, W.A., Oxy-radicals and related species: their formation, lifetimes, and reactions. *Annu. Rev. Physiol.* 1986, **48**, 657 – 667.
42. Branco, M.R., H.S. Marinho, L. Cyrne, and F. Antunes., Decrease of H<sub>2</sub>O<sub>2</sub> plasma membrane permeability during adaptation to H<sub>2</sub>O<sub>2</sub> in *Saccharomyces cerevisiae*, *J. Biol. Chem.*, 2004, **279**, 6501 – 6506.
43. Delaunay A, Pflieger D, Barrault MB, Vinh J., Toledano MB, A thiol peroxidase is an H<sub>2</sub>O<sub>2</sub> receptor and redox-transducer in gene activation., *Cell*, 2002, **111**, 471-481.
44. D. Azevedo, F. Tacnet, A. Delaunay, C. Rodrigues-Pousada, M.B. Toledano Two redox centers within Yap1 for H<sub>2</sub>O<sub>2</sub> and thiol-reactive chemicals signaling., *Free Radic Biol Med*, 2003, **35**, 889-900.
45. K. Gulshan, S.A. Rovinsky, S.T. Coleman, W.S. Moye-Rowley, Oxidant-specific folding of Yap1p regulates both transcriptional activation and nuclear localization *J Biol Chem.*, 2005, **280**, 40524-40533.
46. M. Gutscher, M.C. Sobotta, G.H. Wabnitz, S. Ballikaya, A.J. Meyer, Y. Samstag, T.P. Dick, Proximity-based protein thiol oxidation by H<sub>2</sub>O<sub>2</sub>-scavenging peroxidases, *J Biol Chem*, 2009, **284**, 31532-31540.
47. E.A. Veal, S.J. Ross, P. Malakasi, E. Peacock, B.A. Morgan, Ybp1 is required for the hydrogen peroxide-induced oxidation of the Yap1 transcription factor, *J Biol Chem*, 2003, **278**, 30896-30904.
48. Samuni, A.; Aronovitch, J.; Godinger, D.; Chevion, M.; Czap-ski, G., On the cytotoxicity of vitamin C and metal ions. A site- specific Fenton mechanism. *Eur. J. Biochem.* 1983, **137**, 119-124.
49. Levine, R.L.; Garland, D.; Oliver, C.N.; Amici, A.; Climent, I.; Lenz, A.-G.; Ahn, B.-W.; Shaltiel, S.; Stadtman, E.R., *Determination of carbonyl content in oxidatively modified proteins. Meth. Enzymol.*, 1990, **186**: 464-478.
50. Canfield, R.E. and Liu, A.K., *J. Biol. Chem.* 1965, **240**, 1997-2002.
51. Voet, D. and Voet, J., “*Biochemistry*”, John Wiley & Sons Inc. 2011, **4**, 517-525.

52. Madhuri M. Ugrankar, G Krishnamoorthy, Bala S. Prabhannanda, *J. Biosci.* 1991, **16**, 21-28.
53. Vad R, et al. Engineering of a *Pichia pastoris* Expression System for Secretion of High Amounts of Intact Human Parathyroid Hormone. *J. Biotechnol.*, 2005, **116(3)**, 251–260.
54. Hagenson MJ. Production of Recombinant Proteins in the Methylophilic Yeast *Pichia pastoris*. *Bioprocess Technol.*, 1991 **12**, 193–212.
55. Shugar D., *Biochimica et Biophysica Acta.*, 1952, **8**, 302-309.
56. K.M. Zsebo, H.S. Lu, J.C. Fieschko, L. Goldstein, J. Davis, K. Duker, S.V. Suggs, P.H. Lai, G.A. Bitter, Protein secretion from *Saccharomyces cerevisiae* directed by the prepro-alpha-factor leader region, *J. Biol. Chem.* **261** (1986) 5858–5865.
57. R. Couderc, J. Baratti, Oxidation of methanol by the yeast *Pichia pastoris*: purification and properties of the alcohol oxidase, *Agric. Biol. Chem.* **44** (1980) 2279–2289.
58. Brierley, et al., 1994; Siegel, et al., Heavy metal biosorption sites in *Aspergillus niger*. *Bioresource Technology.* **61**(1997). 221-227.
59. Tashiro K, Nakamura T, Honjo T. The signal sequence trap method. *Method Enzymol.* 1999; **303**:479–95.
60. Cereghino JL, Cregg JM. Heterologous protein expression in the methylophilic yeast *Pichia pastoris*. *Fems Microbiol Rev.* 2000;**24(1)**:45–66.
61. Basco RD, Cueva R, Andaluz E, Larriba G. In vivo processing of the precursor of the major exoglucanase by KEX2 endoprotease in the *Saccharomyces cerevisiae* secretory pathway. *Bba-Mol Cell Res.* 1996;**1310(1)**:110–8.
62. Schechter I, Berger A. On the size of the active site in proteases. I. papain (Reprinted from *Biochemical and Biophysical Research Communications*, vol 27, pg 157, 1967). *Biochem Biophys Res Co.* 2012;**425(3)**:497–502.
63. Germain D, Thomas DY, Boileau G. Processing of Kex2 pro-region at two interchangeable cleavage sites. *FEBS Lett.* 1993;**323(1–2)**:129–31.
64. Rholam M, Brakch N, Germain D, Thomas DY, Fahy C, Boussetta H, et al. Role of Amino-Acid-Sequences Flanking Dibasic Cleavage Sites in Precursor Proteolytic Processing—the Importance of the First Residue C-Terminal of the Cleavage Site. *Eur J Biochem.* 1995;**227(3)**:707–14.

65. Mehmedalijia J, Wallberg F, Bollok M, Garcia P, Enfor S, *Microbial Cell Factories*, 2003, **2**: 6.
66. Huang et al., Yeast Secretion Dynamics, *Biotechnology and Bioengineering*. 2008, **101**: 1264-1275.
67. Saito, A., Sako, Y., Azakami, H., and Kato, A. (2003) “functional Properties of Glycosylated Lysozyme Secreted in *Pichia Pastoris*”, *Biosci. Biotechnol. Biochem.* **67**(11), 2334-2343.